universität wien

DIPLOMARBEIT

Titel der Diplomarbeit

Investigations into the interaction between the β-secretase protein BACE1 and a member of the reticulon family, RTN3.

angestrebter akademischer Grad

Magistra der Pharmazie (Mag.pharm.)

Verfasserin / Verfasser:	Christine Weber
Matrikel-Nummer:	0304331
Studienrichtung /Studienzweig (lt. Studienblatt):	Pharmazie
Betreuerin / Betreuer:	O. Univ.-Prof. Dipl.-Ing. Mag. Dr. Christian Noe

Wien, im März 2010

ACKNOWLEDGMENT

First and foremost I'd like to thank O.Univ.Prof.Dr. Christian Noe for the supervision of this project at the University of Vienna and for guidance and critical annotations.

I would like to express the deepest appreciation to Prof. Colin Dingwall, my main supervisor at King's College where I completed all the laboratory-based work. Without his mentorship and his many valuable suggestions during the experiments and the writing process this diploma thesis would not have been possible.

Many thanks go in particular to Dr. Ruth Rose for sharing her extensive knowledge in Protein Biochemistry with me, sparking my interest in the research problem and inspiring me to look at it from different perspectives to find new approaches. I also benefited a lot from insightful discussions with Dr. Mary Hughes who kindly granted me advice whenever problems arose with my tissue cultures or in general concerns.

I thank the Chemical Biology research group at King's College for providing all the equipment I needed to produce and complete my thesis.

I gratefully thank Dr. Glyn Steventon and Selina Lovell for the excellent Erasmus coordination and administrative help in London. My special thanks go to my Erasmus Coordinator in Vienna, Ass-Prof.Dr. Hannelore Kopelent, who has been priceless in organising my stay abroad, providing information and encouragement and for being my first place to go whenever I had questions. In addition, I would like to thank her and Dr. Winfried Neuhaus for critical reading of this thesis and insightful discussions.

Thanks to my friends at both Universities, especially Sebastian and Jeehyea, for encouragement, advice and a great time we spent together. To my friends outside the lab world – it felt great to have your support and belief in me.

Finally, I thank my family for supporting me throughout my studies at University and providing the foundation I needed to complete this work.

ABSTRACT

As the number of cases of Alzheimer's disease (AD) is constantly rising in all developed countries, the unmet medical need for a curative treatment continues to grow. Current drugs improve symptoms, but do not have profound disease-modifying effects. The generation and aggregation of β-amyloid peptides (Aβ), proteolytic derivatives of amyloid precursor protein (APP), is believed to play a key role in the onset and progression of AD. Consequently, inhibition of the major APP cleaving enzyme, BACE1 (β-site APP cleaving enzyme), is generally recognised as a promising therapeutic strategy and currently an active area of investigation. A wide variety of BACE1 inhibitors have been reported so far. Among them is Reticulon 3 (RTN3), which was recently proposed to act as a natural cellular modulator of BACE1 activity.

This study focused particularly on the interaction between BACE1 and RTN3, aiming to reconstitute the original approach and confirm binding between the two proteins. When using a transiently transfected neuroblastoma cell line binding assays did not show the proposed interaction. In a different approach, representing a fundamental part of the project, RTN3 was successfully cloned and expressed recombinantly. A systematic method was devised to combine both protein purification and binding studies of RTN3 and BACE1.

Surprisingly, my findings indicated that the proposed interaction cannot be reconstituted using recombinant proteins.

ZUSAMMENFASSUNG

Mit steigender Prävalenz von Morbus Alzheimer in den Industrienationen wird auch die bisher erfolglose Suche nach einer effektiven Pharmakotherapie immer dringlicher. Gegenwärtig verfügbare Medikamente verbessern zwar die Symptomatik, haben jedoch keinerlei Auswirkungen auf das Fortschreiten der Krankheit. Eine allgemein anerkannte Schlüsselfunktion in der Alzheimer-Pathogenese nimmt dabei die Produktion und Aggregation des Amyloid-β (Aβ) Peptids ein, eines proteolytischen Derivats des Vorläufers Amyloid Precursor Protein (APP). Aus diesem Grund erscheint die Inhibition des APP spaltenden Enzyms, BACE1 (β-site APP cleaving enzyme), als eine aussichtsreiche Strategie in der Therapie der Krankheit und ist derzeit Gegenstand intensiver wissenschaftlicher Forschung. Eine Vielzahl an BACE1 Inhibitoren wurde bereits identifiziert. Unter ihnen auch Reticulon 3 (RTN3), das erst kürzlich als zelleigener BACE1 Modulator vorgeschlagen wurde.

In der vorliegenden Arbeit wurde die Interaktion zwischen BACE1 und RTN3 untersucht, mit dem vorrangigen Ziel, die bereits publizierte Methode zu überprüfen, zu validieren und die postulierte Protein-Protein Bindung zu bestätigen. Im ersten Teil der Arbeit wurde mit einer humanen Neuroblastom-Zelllinie gearbeitet. Eine transiente Transfektion mit RTN3 und darauf folgende Interaktionsstudien brachten jedoch keine positiven Resultate. In einem alternativen Versuch wurde RTN3 in einen bakteriellen Vektor integriert und rekombinantes Protein exprimiert, mit dem die Interaktionsstudien durchgeführt wurden. Dabei wurde eine neue Methode entwickelt, um die Proteinaufreinigung mit Bindungsstudien zwischen RTN3 und BACE1 zu kombinieren.

Allerdings konnte mit Hilfe des rekombinanten Systems die Interaktion zwischen den beiden Proteinen nicht bestätigt werden.

TABLE OF CONTENTS

ABBREVIATIONS

5Y°	SH-SY5Y neuroblastoma cells
Aβ	Amyloid beta
AD	Alzheimer's disease
ADAM	A disintegrin and metalloproteinase domain
APP	Amyloid precursor protein
BACE1	β-site APP cleaving enzyme 1
BSA	Bovine serum albumine
CMC	Critical micelle concentration
CTF	C-terminal fragment
dH_2O	Distilled water
ddH_2O	Double-distilled water
DMEM	Dulbecco's minimal essential medium
DTT	Dithiothreitol
ECL	Enhanced chemiluminescence
EDTA	Ethylenediaminetetraacetic acid
ER	Endoplasmic reticulum
FAD	Familial Alzheimer’s disease

FBS	Foetal bovine serum
FPLC	Fast protein liquid chromatography
GST	Glutathion-S-Transferase
HPLC	High performance liquid chromatography
IP	Immunoprecipitation
IPTG	Isopropyl β-D-1-thiogalactopyranoside
LB	Luria Bertani Broth
MAB	Monoclonal antibody
MBP	Maltose binding protein
µl	Microlitre
ml	Millilitres
mM	Millimolar
MW	Molecular weight
PBS	Phosphate-buffered saline
PBST	PBS containing 0.05 % Tween 20
PCR	Polymerase chain reaction
RHD	Reticulon Homology Domain
rpm	Rotations per minute
RTN	Reticulon
RTN3 HD	Reticulon 3 Homology Domain
SEC	Size exclusion chromatography
SDS	Sodium dodecyl sulfate

SDS-PAGE	Sodium dodecyl sulfate polyacrylamide gel electrophoresis
TE	Tris-EDTA
TEMED	N,N,N',N'-Tetramethylethylenediamine
TRIS	Tris(hydroxymethyl)aminomethane

CHAPTER 1

INTRODUCTION

1.1. Alzheimer's disease

Alzheimer's disease (AD) is the most common cause of neurodegenerative dementia in the elderly (*Francis et al., 1999*). With the increasing longevity of our population, AD is already approaching epidemic proportions (*Brookmeyer et al., 2007*) with no cure or preventative therapy yet available. AD is a progressive and ultimately terminal brain disorder characterised pathologically by extracellular deposits of β-amyloid plaques, intracellular formation of neurofibrillary tangles and neuronal loss.

The rare form of familial Alzheimer's disease (FAD) has been identified to have a genetic link. It is inherited in an autosomal dominant fashion. All cases known so far have an early onset (< 65 years), and as many as 50 percent are now known to be caused by defects in three genes located on three different chromosomes. However, the more common form is sporadic AD, where no obvious inheritance pattern is seen and which tends to occur later in life.

1.2. Pathology & Causes of AD

Despite extensive study the exact etiology of AD still remains to be identified. However, three major hypotheses have been proposed to clarify the cause of the disease. The *cholinergic hypothesis* postulates a connection between some of the cognitive impairments of AD and a disturbance in cerebral cholinergic neurotransmission. Support for this theory came in the mid-1970s with reports of extensive neocortical deficits in the enzyme responsible for the synthesis of acetylcholine, choline acetyltransferase (*Davies et al., 1976; Perry et al., 1977*). Subsequent studies confirmed a substantial presynaptic cholinergic deficit due to

reduced choline uptake (*Rylett et al., 1983*), acetylcholine release (*Nilsson et al., 1986*) and loss of cholinergic neurons (*Whitehouse et al., 1982*). At this time research also suggested an emerging role of acetylcholine in learning and memory (*Drachman et al., 1974*). Considering these observations it was proposed that degeneration of cholinergic neurons and the associated loss of cholinergic neurotransmission in the cerebral cortex contributed significantly to the deterioration in cognitive function seen in AD patients (*Bartus et al., 1982*). This hypothesis marked the very beginning of systematic biochemical investigations into the mechanisms of AD. Although many studies have challenged the veracity of the cholinergic hypothesis as an explanation for AD in the past 20 years, the theory has led to the discovery of several treatment targets that are still valid. Cholinesterase inhibitors play an important role in therapeutic treatment nowadays, and even though they are not a curative treatment they do allow the alleviation of some clinical symptoms.

The second hypothesis is linked to the intracellular deposition of hyperphosphorylated tau. According to the *tau hypothesis* cognitive impairment correlates with abnormal aggregation of tau, a microtubule-associated protein expressed in neurons which stabilises microtubules in the cell cytoskeleton. In AD patients, hyperphosphorylated tau accumulates as paired helical filaments (*Goedert et al., 2006*) that consecutively aggregate into neurofibrillary tangles inside nerve cell bodies (*Goedert et al., 1991*). These tangles tend to associate with amyloid plaques, cause the microtubules to disintegrate and later induce a complete breakdown of the cellular transport system (*Iqbal et al., 2005*). The malfunctions in biochemical communication between neurons typically precede the death of the cell.

The *amyloid hypothesis* proposes an early and crucial role of Amyloid β-peptide (Aβ) in initiating the pathogenic cascade of AD. It argues that the neurodegenerative progression, as well as the development of neurofibrillary tangles, is a consequence of an imbalance between the production and clearance of Aβ (*Hardy & Selkoe, 2002; Annaert & De Strooper, 2002*). Further details on Aβ generation and function will be provided in section 1.4. An increase in Aβ production enhances oligomerisation and leads to the formation of plaques, consequently inducing neurotransmitter deficiency and neuronal damage leading to cell death.

So far, no single pathological lesion can explain all of the hallmarks of AD. There have been major debates as to whether amyloid plaques or neurofibrillary tangles occur first in AD pathology (*Selkoe, 2001*). However, genetic and pathological evidence strongly supports the amyloid cascade hypothesis (*Citron, 2004*), which I will elaborate on in the following sections.

Further to the presented major hypotheses a variety of additional explanatory models has been published so far. Several inflammatory processes, mitochondrial dysfunction, metabolic disturbances and alterations in Insulin signalling, the loss of calcium regulation and defects in the cholesterol metabolism have been suggested to be relevant in the progress of AD (*Querfurth et al., 2010*).

1.3. Genetics of AD

The vast majority of AD cases are sporadic with no apparent genetic linkage. However, the growing understanding of the underlying genetic principles has been essential in uncovering some of the cell and molecular processes leading to the disease state. Genetic investigations started in 1981, when *Heston et al.* observed a high incidence of AD-type neuropathology in patients suffering from Down's syndrome (trisomy 21). A possible genetic link between AD and an abnormal gene or structural defect on chromosome 21 seemed logical. This was later confirmed when the gene encoding the amyloid precursor protein (APP) was isolated and mapped to chromosome 21 (*Goldgaber et al., 1987; Kang et al., 1987; Robakis et al., 1987; Tanzi et al., 1987*). In the following years several mutations were found in APP, accounting for approximately 5-20 % of published cases of early-onset FAD (*Tanzi et al., 1992; Campion et al., 1996*). Efforts were turned towards the identification of other genes involved, and in 1995, presenilin 1 and 2 (*PS-1*; *PS-2*) were reported as novel FAD related genes on chromosome 14 and 1, respectively (*Sherrington et al. 1995; Levy-Lahad et al., 1995*). The majority of mutations discovered on both presenilins and APP have been shown to increase the ratio of cerebral Aβ (*Scheuner et al., 1996; Price et al., 1998*), in particular the more fibrillogenic form of the peptide, $A\beta_{42}$ (*Jarrett et al., 1993*). To date, a total of 32 rare, autosomal-dominant mutations have been found in APP, 176 in PS-1 and 14 in PS-2 (http://www.molgen.ua.ac.be/ADMutations/), assigning in particular PS-1 a major role in contributing to early-onset

AD risk. However, there is still no evidence that genetic variants of the presenilins are associated with increased late-onset AD susceptibility.

A genetic model to explain late-onset AD (> 65 years) was devised, when *Pericak-Vance*, in 1991, reported a significant genetic linkage to the gene encoding apolipoprotein E (APOE), an apoprotein enhancing proteolytic break-down of Aβ. The polymorphism ε4 was identified to represent a major risk factor for the development of late-onset AD (*Schmechel et al., 1993; Strittmatter et al., 1993*). However, it is not a determinant of the disease as at least a third of AD patients are *ApoE4* negative and some *ApoE4* homozygotes never develop the disease.

1.4. Aβ pathways & APP processing

The *Amyloid cascade hypothesis* proposes an accumulation of Aβ deposits as the initial cause for AD. Aβ, between 39 to 43 amino acids in length, is formed after sequential cleavage of the amyloid precursor protein (APP). APP is a transmembrane glycoprotein of as yet undetermined function, which is ubiquitously expressed throughout the body (*Ling et al., 2003*) and can be processed by two major different pathways (Figure 1.1).

The first pathway is the non-amyloidogenic α-secretory pathway where APP is firstly cleaved by α-secretase to produce soluble sAPPα and the carboxy-terminal fragment, C83. This membrane embedded C83 fragment is further cleaved intramembranously by γ-secretase, releasing the non-pathogenic p3 peptide into the extracellular space.

Alternatively, APP cleavage can occur via the pathological amyloidogenic β-secretory pathway. Here, initial cleavage is catalysed by β-secretase, resulting in the release of the sAPPβ fragment and leaving the membrane-bound C-terminal fragment C99. The C99 domain is cleaved within the cell membrane by γ-secretase to create pathogenic Aβ (*De Strooper & Annaert, 2000; Koo, 2002*) and AICD. There are two major forms of Aβ: the more abundant and soluble 40 amino acid fragment and the pathogenic 42 amino acid isoform, $A\beta_{42}$ (*Jarrett et al., 1993*). AICD is released into the cytoplasm and targeted to the nucleus, signalling transcription activation.

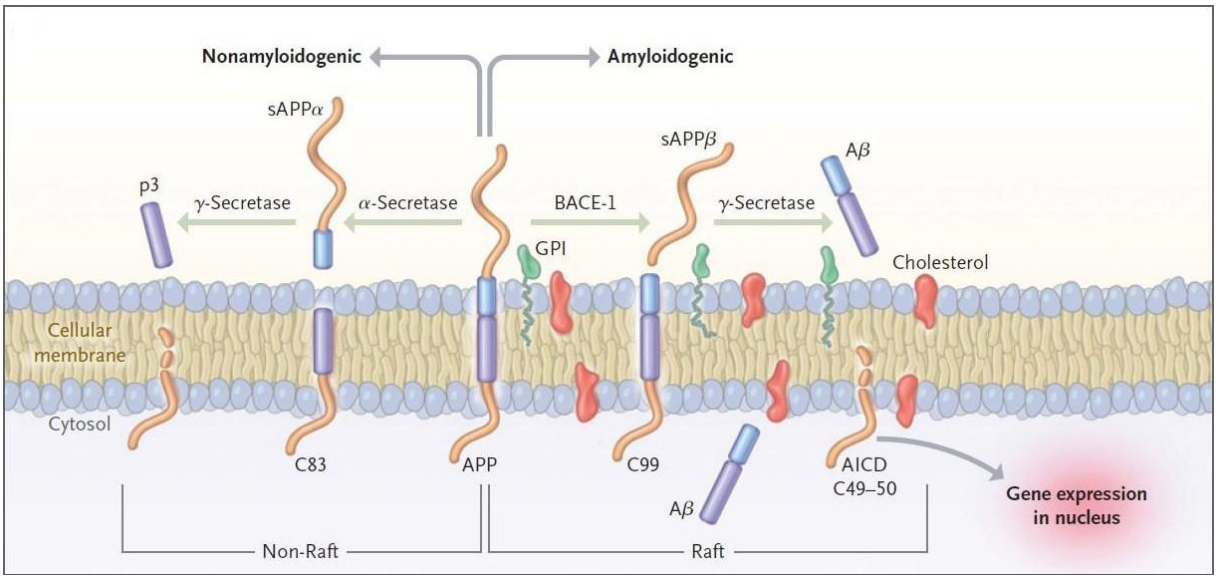

Figure 1.1: Processing of Amyloid Precursor Protein.
In the α-secretory pathway APP is cleaved by α-secretase and γ-secretase to form sAPPα, AICD and the non-pathogenic P3. In the β-secretory pathway APP is processed by β-secretase (BACE1) and γ-secretase to produce sAPPβ, AICD and amyloid plaque-causing Aβ. Lipid rafts are membrane micro-environments enriched in sphingomylelin, cholesterol, and glycophosphatidylinositol (GPI)–anchored proteins. They play a major role in the assembly of β- and γ-secretases and the processing of APP into Aβ.
(Figure according to Querfurth et al., 2010)

1.5. AD associated secretases

α-secretase

Several proteins with α-secretase-like activity have been identified to date (*Ling et al., 2003; Dillen & Annaert, 2006*). The majority of candidates belong to the ADAM ("a disintegrin and metalloproteinase domain") family. Those expected to be of relevance in AD are the two metalloproteinases ADAM10 and ADAM17 (TACE) which have been shown to act as α-secretases (*Allinson et al., 2003*). Another protease that may cleave APP at the α-secretase site is BACE2 (β-site APP-cleaving enzyme 2), a homologue of the β-secretase enzyme BACE1. However, the function of BACE2 as either an α- (*Yan et al., 2001; Basi et al., 2003*) or β-secretase (*Hussein et al., 2000; Yan et al., 1999*) has not yet been fully defined. Furthermore, low levels of expression in the brain suggest it might play a rather unimportant role (*Vassar et al., 2002).*

γ-secretase

The γ-secretase intramembraneous protease complex is responsible for the final cleavage of APP resulting in the release of p3 peptide or Aβ. The complex is composed of 4 individual proteins: presenilin (PS), nicastrin (NCT), anterior pharynx-defective 1 (APH-1) and presenilin enhancer 2 (PEN-2). PS is an aspartyl protease and the catalytic subunit of γ-secretase. *Kaether et al.*, in 2006, developed a model of complex assembly in which NCT and APH-1 stabilise PS before PEN-2 is added as the last component to complete the complex. PEN-2, among other possible roles, helps to stabilise the complex after PS proteolysis has generated the activated N- and C-terminal fragments of APP (*Prokop et al., 2004*).

β-secretase

Proteolytic processing of APP at the β-site is essential in the generation of Aβ. The major β-secretase in the brain is a type 1 membrane-associated aspartyl protease of 501 amino acids, called β-site APP-cleaving enzyme 1 (BACE1; *Hussain et al., 1999; Sinha et al., 1999; Vassar et al., 1999; Yan et al., 1999*). Like many other proteases, BACE1 is produced as a pro-enzyme predominantly within the endoplasmic reticulum (ER) and the nuclear envelope and is trafficked through the Golgi to the cell surface during which it is post-translationally modified. The mature enzyme exhibits complex N-glycosylation and three intramolecular disulfide-bonds, which are critical but not essential for APP processing (*Fischer et al., 2002*). Three cysteine residues within the cytosolic tail of BACE1 are palmitoylated, which may influence intracellular localisation or trafficking (*Benjannet et al., 2001*).

BACE1 is the rate-limiting enzyme in the formation of Aβ (*Vassar, 2001*). Over-production of BACE1 in cell cultures enhanced the quantity of β-secretase cleavage products (*Vassar et al., 1999*). More importantly, a transgenic mouse line expressing human BACE1 induced the amyloidogenic processing of APP and elevated $A\beta_{42}$ levels (*Bodendorf et al., 2002*). Knocking out the BACE1 gene completely impaired the β-secretase cleavage of APP and diminished the production of Aβ (*Cai et al., 2001*). Surprisingly, BACE1 deficient mice developed normally and showed no phenotypic alterations despite an abolished β-secretase activity in the brain (*Luo et*

al., 2001; Roberds et al., 2001). This indicates that BACE1 might be dispensable for normal development and physiological functions *in vivo*. Moreover, elevated BACE1 has been observed in the brains of individuals with sporadic AD (*Holsinger et al., 2002; Fukumoto et al., 2002; Yang et al., 2003*). The inhibition of BACE1 activity therefore seems to be a promising therapeutic strategy in the treatment of AD (*Citron, 2004*).

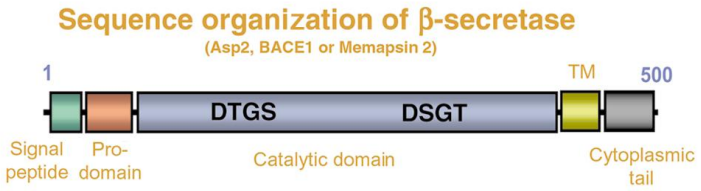

Figure 1.2: Sequence organisation of β-secretase.
BACE1 has a cleaved signal peptide, a prodomain and a catalytic domain which contains the catalytic aspartic residues. The catalytic domain comprises 3 di-sulfide bridges which is characteristic for aspartic proteinases and is glycosylated at 4 sites. The cytoplasmic tail contains a di-leucine endosomal retreival signal, palmitoylated cysteine residues and phosphorylation sites. (Colin Dingwall, 2001: Spotlight on BACE)

1.6. Reticulons as BACE1 inhibitors

The concept of β-secretase inhibition seems to be a promising line of inquiry in the treatment of AD. However, inhibitor development has proved challenging. For aspartic proteases, potent and specific peptidic inhibitors can usually be identified, but the transition to small drug-like molecules with the desired pharmacokinetics and the ability to penetrate the blood-brain-barrier remains difficult (*Vassar, 2002*). Over the past few years a wide variety of BACE1 inhibitors have been reported, many of them were designed as peptidomimetic inhibitors based on transition-state analogues (*Kimura et al., 2006*).

An alternative approach to inhibit BACE1 was the identification of natural cellular modulators of BACE1 activity. For instance, it has been demonstrated that BACE1 activity is regulated by the level of glycosylation (*Charlwood et al., 2001*), composition of lipids in the membrane bilayer (*Kalvodova et al., 2005*), interactions with heparin sulphate (*Scholefield et al., 2003*) and, more recently, the reticulon proteins. In 2004, *He et al.* used a coimmunoprecipitation approach to search for

cellular proteins that interact with BACE1 and reported the identification of reticulon family members as binding partners and inhibitors of BACE1.

Reticulons (RTNs) are a group of integral membrane proteins that are largely localised in the endoplasmatic reticulum (ER) and exist in plants, fungi and animals (*Oertle et al., 2003a*). While the precise cellular functions remain to be defined, RTNs have been shown to regulate many different cellular processes. They have also been demonstrated to interact with diverse cellular proteins, extracellular receptors (*Fournier et al., 2001*), fusion and endocytic proteins (*Oertle et al., 2003a*). In mammalian genomes, four independent reticulon genes - *RTN1, RTN2, RTN3* and *RTN4* - have been identified to encode a large number of gene products with multiple spliced variants. While the exact functions of RTN1 to RTN3 are unknown, research has revealed a significant role of RTN4, also known as Nogo, in regulatory processes in the mammalian central nervous system. The subform RTN4-A has been shown to inhibit neurite outgrowth and cell spreading *in vitro* (*Oertle et al., 2003b*), preventing the regeneration of lesioned nerve fibers in the brain (*Chen et al., 2000*).

All RTNs are composed of a completely divergent N-terminal domain, and a highly conserved RTN homology domain (RHD), unique to this family of proteins (*Yang and Strittmatter, 2007*). The conservation of the RHD has already been shown to confer common functions upon RTNs, such as localising RTNs to the appropriate membranes and/or mediating protein interactions (*Yan et al., 2006*). As previously mentioned all RTN members were shown to interact with BACE1, implying that the conserved RHD may mediate binding of RTNs to BACE1. This study focused in particular on RTN3 because of its strong inhibitory effects on enzyme activity and high expression by neurons (*He et al., 2004*).

1.7. RTN3: structural organisation and binding to BACE1

Among all reticulon family members RTN3 showed the highest expression in mouse and human post-mortem brain. In the latter it was predominantly expressed in gray matter and enriched in neuronal cell bodies. It is localised primarily in the ER and the Golgi (*He et al., 2004; Wakana et al., 2005*). However, it was also found in axons, dendrites, and the growth cone (*Hu et al., 2007*). BACE1, although being ubiquitously present in all brain regions, shows a substantially higher expression in neurons (*Vassar et al., 1999*), similar to RTN3. All this data indicates that RTN3 is more likely to be related to Aβ production in human brain than other RTN members. On a cellular level, interaction is expected to take place in both the ER and Golgi or Trans-golgi-network (TGN) compartments, as both proteins have been successfully co-localised there (*He et al., 2004*).

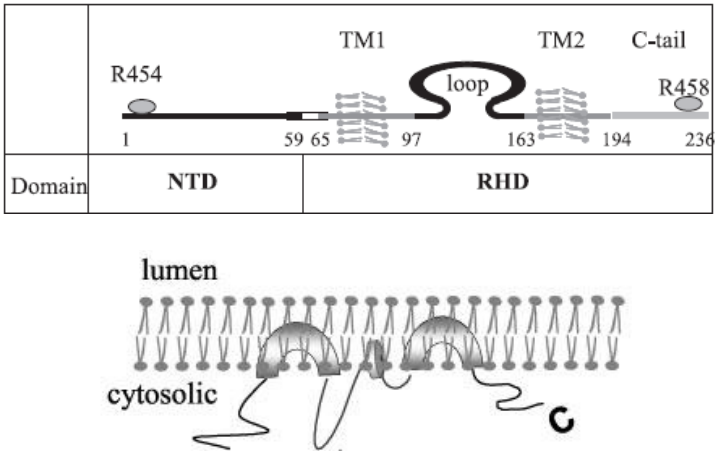

Figure 1.3: Structural organisation of RTN3.
A schematic diagram of full-length RTN3 (236 aa), showing transmembrane regions (TM), whereas TM1 governs insertion of RTN3 into the membrane, the loop and C-terminal tail. Below is the predicted membrane topology of RTN3. All figures according to He et al., 2007.

As illustrated in figure 1.3 RTN3 adopts a ω-shape membrane topology with both the N- and C-terminal ends retained on the cytosolic side. Like other members of the reticulon family RTN3 has two major domains: an unique N-terminal domain (NTD) and the C-terminal RHD. The latter includes two long hydrophobic stretches (28-36 amino acids) that are separated by a 66 amino acid loop, and a C-terminal tail. The two putative transmembrane (TM) domains embed RTN3 in the membrane and have been shown to be critical components for the function of RTNs. Disruption of the TM1 domain prevents integration of RTN3 into the membrane, suggesting that proteins

are perhaps misfolded and degraded in cells. RTN3 mutants with disruption or deletion in either TM1 or TM2 also fail to interact with BACE1 as the binding domain is probably buried due to different protein folding (*He et al., 2007*).

The exact region mediating the binding of RTN proteins to BACE1 has been mapped to the C-terminal tail, in particular a highly conserved triplet amino acid QID motive that is shared among all RTN members (*He et al., 2006*). According to these observations proper integration of RTN3 into the lipid bilayer as well as optimal conformation of transmembrane regions and the C-terminal tail containing the conserved QID motive are essential for the binding of RTN3 to BACE1.

From the BACE1 perspective binding is mediated by the C-terminal region, with those sequences immediately adjacent to the transmembrane domain (TM) being of substantial importance for successful interaction. The topological orientation is consistent with the location of the RTN3 QID motif. Both regions face the cytoplasmic side, allowing direct contact. Similar to the observations made for RTN3, the appropriate orientation of BACE1 within the membrane seems to be important, although the BACE1 TM alone is insufficient for interaction with RTN3 (*He et al., 2006*).

CHAPTER 2

AIMS AND OBJECTIVES

BACE1 is widely recognised to be one of the most promising drug targets for inhibition of Aβ generation. Various approaches for inhibiting BACE1 have already been actively pursued and the identification of RTN3 as a BACE1 modulator offers an alternative possibility to discover small molecules that could mimic inhibitory effects. To study this potential regulatory mechanism in molecular detail it is essential to establish a method to reconstitute the BACE1-RTN3 binding *in vitro*.

CHAPTER 3

MATERIALS & METHODS

3.1. Materials & Chemicals

All chemicals were purchased from Sigma-Aldrich Ltd (Poole, UK) unless stated otherwise.

3.2. Cell Culture

3.2.1. Cells

The cells used in this study were stably transfected SH-SY5Y cells. SH-SY5Y (5Y°) is a human neuroblastoma cell line and was purchased from ATCC. The *BACE1-MYC* vector (C-terminally tagged) was prepared by Emma Gray at the Institute of Psychiatry (King's College, London) and the stable cell line was created by Dr Ruth Rose (King's College, London).

3.2.2. Solutions

All solutions mentioned in this section were purchased from Invitrogen unless stated otherwise.

- ***Medium***

  Dulbecco's Modified Eagle Media (DMEM), supplemented with

Fetal Bovine Serum (FBS)	10 %
Glutamine	2 mM
G418	2 mM

- ***Trypsin/EDTA 10x***

Trypsin	0.25 %
EDTA	0.53 mM

3.2.3. Propagation and splitting of cells

Cells were cultured in T-75 flasks at 37 °C with 95 % air, 95 % humidity and 5 % CO_2. Once a cell-confluency between 80 to 90 % was reached, the culture was split in order to achieve continuous growth. The medium was removed from the T-75 flask using a vacuum aspirator and 5 ml of 10x Trypsin/EDTA was added to detach adherent cells from the flask surface. Remaining cells were detached by knocking. After 5 minutes incubation at 37 °C 1 ml of FBS was added to stop Trypsin/EDTA from acting on the cells. The cells were pelleted by centrifugation at 2,000 rpm for 5 minutes. The supernatant was aspirated and the cells resuspended in 5 ml of medium. A 1 ml aliquot was removed and pipetted into a new T-75 flask containing 10 ml of medium. The remaining 4 ml of suspension were, if needed, used to grow larger cultures in T-175 flasks along with 15 ml of medium. Cells were regularly observed under a microscope to control appropriate growth.

3.2.4. Harvesting cells (T-175)

Fully confluent T-175 cells were harvested with 10 ml of Trypsin/EDTA and after 5 minutes 2 ml of FBS as described in section 3.2.3. The cells were pelleted by centrifugation at 2,000 rpm for 5 minutes; the pellet was resuspended in 1 ml of sterile PBS (Sigma) and then pelleted again. After aspirating the supernatant the pellet was frozen at -80 °C for storage.

3.2.5. Counting cells

To seed an accurate number of cells into a multi-well the cells were harvested with Trypsin/EDTA and FBS as described in section 3.2.3. Cells were pelleted and resuspended in 1 ml of medium. A 10 µl aliquot of the suspension was added to 40 µl of 0.02 % Trypan Blue plus 30 µl PBS in a micro-centrifuge tube. A 10 µl sample of this mixture was directly applied to a haemocytometer. Cells were counted and the concentration of cells in suspension was calculated according to equation 3.1, whereby 8 is the dilution factor and 10^4 is the area coefficient.

$$\textit{Number of cells/ml} = \textit{average cell number of 4x16 squares} \cdot 8 \cdot 10^4 \qquad (3.1)$$

3.2.6. Transfection

5Y^{o} cells overproducing BACE1-MYC were counted as described in section 3.2.5, seeded at a density of 2 x 10^5 cells per well in a 6-well-plate and allowed to grow for 18 hours. In a 1.5 ml micro-centrifuge tube 2 µg of isolated double-stranded plasmid DNA (received from Dr Mitsuo Tagaya, Department of Pharmacy & Life Science at Tokyo University) was suspended in 100 µl of Opti-MEM®. A solution of 10 % Lipofectamine™ in Opti-MEM® was prepared and 100 µl was added to the DNA-Opti-MEM®-mix in the tube. The mixture was flicked gently and incubated at room temperature for 45 minutes. A further 200 µl of Opti-MEM® was added. The medium in the 6-well-plate was removed and to each well 0.4 ml of DMEM and 0.4 ml of DNA-Opti-MEM® mixture were added. The plate was incubated at 37 °C for 6 hours in an incubator. The culture was provided with additional 0.8 ml of medium containing 10 % extra FBS (20 % in total) and left for another 3 days in the incubator to grow.

3.3. Molecular Biology Methods

All general nucleic acid protocols were carried out as described in Laboratory Manuals (Sambrook *et al.* 2001).

3.3.1. Materials

Bacterial strains

Strains	Genotype	Description	Source
JM109	*end*A1, *rec*A1, *gyr*A96, *thi*, *hsd*R17 (rk^-, mk^+), *rel*A1, *sup*E44, Δ(*lac*$^-$ *pro*AB), F', *tra*D36, *pro*AB, *laq*I^{q}ZΔM15	*Lac* promoter	Promega
BL21-Codonplus(DE3)-RIL	*E. coli B F– ompT hsdS(r_B– m_B–) dcm$^+$ Tetr gal λ(DE3) endA Hte [argU ileY leuW Camr]*	IPTG inducible, T7 promoter	Stratagene

Table 3.1. *The complete list of bacterial E.coli strains used during this study.*

Plasmids

Plasmids carrying the *BACE1* gene (pGEX-4T-1-BACE1, amino acids 477-501) were constructed by Dr B. Angeletti as described in Angeletti *et al.* (2005)

Vector	Description	Source
pMal-c2x	Over-expression maltose-binding protein (MBP) fusion vector, Amp^R, *lac* promoter	NEB
pCW01	pMal-c2x containing MBP-fused *RTN3* HD cloned, *Bam*HI, *Hind*III	this study
pGEX-4T-1	High level expression Glutathione-S-transferase (GST) fusion vector, *tac* promoter, *lac* I^q, Amp^R	GE Healthcare
pBA9-pGEX-4T-1	GST-fusion vector, containing the sequence coding for BACE1 amino acids 477-501	Dr B. Angelleti

Table 3.2. *The complete list of vectors used during this study.*

Solutions

- ***Tris-EDTA (TE) Buffer***
  10 µM Tris-HCl pH 8.0
  1 mM EDTA pH 8.0
  Autoclaved

Bioinformatics

The amino acid sequence for RTN3 was obtained from the NCBI website (http://www.ncbi.nlm.nih.gov/). NEBCutter v2.0 (http://tools.neb.com/NEBcutter2) was used to visualise the open reading frames of the DNA sequences and select appropriate restriction enzyme sites. MultAlin was used to generate sequence alignments (http://bioinfo.genotoul.fr/multalin/multalin.html.)

3.3.2. Polymerase Chain Reaction

The PCR was carried out in a 2720 Thermal cycler (Applied Biosystems, USA). All solutions and buffers were purchased from Invitrogen unless stated otherwise.

3.3.2.1. PCR for DNA Amplification

According to the instruction manual for Platinum® Taq Polymerase (Invitrogen) all reagents were prepared in a sterile PCR tube as stated in Table 3.3 and gently flicked.

Reagent	***Volume (µl)***
10x PCR Reaction Buffer Minus Mg^{2+}	5
10 mM dNTPs	1
50 mM $MgCl_2$	1.5
10 µm 5' primer	1
10 µm 3' primer	1
ddH_2O	39.3
Template DNA	1
Platinum® *Taq* DNA Polymerase	0.2

Table 3.3. *Components used for DNA Amplification.*

The reaction took place under the following conditions:

PCR Method	1 cycle	activation	2 mins	94°C
	35 cycles	denaturing	30 sec	94°C
		annealing	30 sec	53°c
		elongation	10 sec	72°C
	4°C store overnight			

The complete pFLAG-*RTN3*-CMV-6c template was received from Dr Mitsuo Tagaya at Tokyo University, Department of Pharmacy & Life Science. The Primers were designed to replicate the C-terminal homology domain of *RTN3* (RTN3 HD). Restriction sites for *Bam*HI and *Hind*III were incorporated into the primers (Table 3.4) to allow the gene to be inserted into the multiple cloning site of the pMal-c2x vector

(Table 3.2). All primers used in this study were purchased from Invitrogen (Paisley, UK), prepared at a stock conc of 100 µM in TE and diluted to 10 µM in TE for use. Reaction products were analysed by agarose gel electrophoresis (section 3.3.3).

Source	5' / 3'	Primer sequence	Restriction site
RTN3 HD	5'	CTG GAT CCT ATG AGA AGT ACA AGA CCC	*Bam*HI
RTN3 HD	3'	CCA AGC TTC CAT GTA CTT ATT CTG CC	*Hind*III

Table 3.4. *Primers used in this study. The forward primer incorporated two additional residues to maintain the reading frame, the BamHI restriction site and 19bp of template RTN3 HD annealing sequence. The reverse primer contained two residues, the HindIII restriction site and 18bp of template RTN3 HD annealing sequence.*

3.3.2.2. Colony PCR

Colony PCR was used to determine whether transformed colonies carried the desired gene. Colonies on the plate were numbered 1-10, stabbed with a 10 µl pipette tip and resuspended in 10 µl of sterile water. A 1 µl aliquot of resuspended colony was added to 9 µl of the PCR Stock Mix (Table 3.5) and the PCR performed as described in section 3.3.2.1. The remaining suspension was stored at -20 °C. A negative control containing only the vector pMal-c2x was prepared the same way. The PCR products were run on a 1 % agarose gel as described in section 3.3.3 and colonies carrying the plasmid with insert were identified by the formation of a 139 bp band, representing the amplified *RTN3* HD.

Reagent	***Volume (µl)***
5x Green GoTaq® Flexi Buffer (Promega)	2
25 mM $MgCl_2$ (Promega)	0.6
10 mM dNTPs	0.2
10 µm 5' primer	0.4
10 µm 3' primer	0.4
ddH_2O	5.4
GoTaq® Flexi DNA Polymerase (Promega)	0.05

Table 3.5. *1x PCR Stock Mix for 31 Colony PCR Reactions.*

3.3.3. Agarose Gel Electrophoresis

Agarose gel electrophoresis was performed to isolate and identify DNA fragments. A 1 % agarose gel was used throughout all studies due to the high resolution of DNA fragments within the desired molecular weight range (0.5 - 7 kb). After an electrical current was applied, negatively charged DNA migrated towards the anode, transporting smaller molecules considerably faster through the polysaccharide matrix and thus separating DNA molecules by size.

Nucleic acids were visualised in the gel by addition of the fluorescent dye ethidium bromide, which intercalates between the bases of the DNA strand. The DNA-dye complex absorbs UV light and emits visible orange light at 590 nm which was observed on an ultraviolet transilluminator. Images were taken using the Syngene Bioimaging System UP-D895.

Methodology

A 1 % agarose gel was prepared by dissolving Agarose (Amresco) in 1x UltraPure™ TAE buffer (Invitrogen). Ethidium bromide was added to a concentration of 0.5 µg/ml and the liquid gel was poured into a casting tray containing a sample comb and left to set evenly. After the gel had solidified, the comb was removed and the gel, still in the tray, was inserted horizontally into the electrophoresis chamber and submerged in 1x TAE Buffer. DNA samples were mixed with DNA loading dye (Promega) and loaded onto the gel. A 100 bp marker (Promega) was used as a reference (Figure 3.1). The gel was run at a current of 95 Volts for 40 minutes and visualised under ultraviolet light (254 nm, high energy).

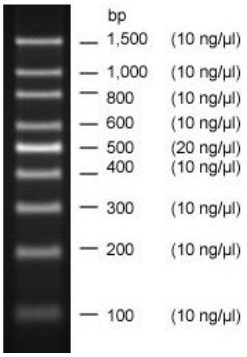

Figure 3.1. *100bp DNA molecular weight marker (Promega)*.

3.3.4. Gel Extraction

To purify the DNA from an agarose gel the QIAquick® Gel Extraction Kit (QIAGEN GmbH) was used. The extraction was completed following the method outlined in the QIAquick® Gel Extraction Kit protocol for micro-centrifuge. The DNA was eluted in 50 µl of Buffer EB into a sterile 1.5 ml micro-centrifuge tube and stored at -20°C.

3.3.5. Restriction Digests

All restriction enzymes and buffers employed here were purchased from Promega.

3.3.5.1. Large scale digests

To digest large quantities of DNA a restriction digest was set up as stated below (Table 3.6). The mixture was incubated at 37 °C for 3 hours to ensure complete digestion.

Reagent	***Volume (µl)***
Extracted DNA	15
ddH_2O	10
*Bam*HI	1
*Hind*III	1
Buffer E (Promega)	3

Table 3.6. *Components used for large scale digests.*

3.3.5.2. Analytical digests

Samples were prepared at the concentrations and with the optimal buffer selected according to the manufacturer's instructions (Table 3.7). The digest was left to incubate at 37 °C for 1 hour and run on a 1 % agarose gel (section 3.3.3).

Reagent	***Volume (µl)***
DNA miniprep/ pMal-c2x	4
Restriction enzyme	0.5
Buffer	1
ddH_2O	4

Table 3.7. *Components used for analytical digests.*

3.3.6. DNA Clean-Up

DNA fragments were purified using Qiagen's QIAquick® PCR Purification Kit Protocol for a micro-centrifuge. The DNA was eluted in 30 µl of Buffer EB into a 1.5 ml micro-centrifuge tube.

3.3.7. Ligation

Digested DNA fragments were ligated using T4 DNA Ligase as stated below (Table 3.8). The ligation product was stored overnight at 4 °C.

Reagent	***Volume (µl)***
2x T4 DNA ligase buffer (Promega)	5
T4 DNA ligase (Promega)	0.5
pMal-c2x digested with *Bam*HI, *Hind*III (vector)	2
Digested DNA fragment (insert)	2.5

Table 3.8. *Components used for ligation.*

3.3.8. Transformation

Competent cells, *BL21-Codonplus(DE3)-RIL,* were slowly defrosted on ice. A maximum volume of 10 % ligation product (for a complete list of all plasmids used see Table 3.2) was added to the cells, mixed carefully and left to stand on ice for 15 minutes. The cells were heat shocked for 50 seconds at 42 °C to ensure the uptake of genetic material and immediately placed on ice for 2 minutes. An aliquot of 200 µl LB was added and cells were allowed to replicate at 37 °C for 1 hour, giving them enough time to produce the newly acquired antibiotic resistance. Cells were spread onto LB-agar plates, containing the required antibiotics, and incubated overnight at 37 °C.

3.3.9. Miniprep

Starter cultures containing 5 ml of LB, antibiotics where required, and a single colony were grown overnight at 37 °C, whilst shaking. The cells were pelleted by centrifugation at 4,000 rpm for 20 minutes at 4 °C. To extract the plasmid DNA from the pellet the QIAquick® miniprep kit for micro-centrifuge (Qiagen GmbH) was used. The DNA was eluted in 50 µl of EB buffer and stored at -20 °C.

3.4. Microbiological Methods

3.4.1. Media for microbiological growth

Tryptone and yeast extracts were purchased from Oxoid Ltd., Hampshire, England. Sources of other materials are stated in the text.

- ***Luria Bertani Broth (LB)***

  NaCl 5 g/L

  Yeast extracts 5 g/L

  Tryptone 10 g/L

  Autoclaved

- ***LB agar***

  Agar in LB 15 g/L

  Autoclaved

- ***Ampicillin***

  10 µg/ml in dH_2O

  Filter sterilised and stored at -20 °C

- ***Chloramphenicol***

  34 µg/ml in 99 % Ethanol

  Stored at -20 °C

- ***Isopropyl β-D-1-thiogalactopyranoside (IPTG)***

  0.4 mM in dH_2O

  Filter sterilised and stored at -20 °C

3.4.2. Production of Recombinant Proteins

The *E.coli* strain *BL21-Codonplus(DE3)-RIL* was transformed (section 3.3.8) with an expression plasmid carrying the desired gene (Table 3.2) and incubated at 37 °C overnight on a LB plate with the required antibiotics. Starter cultures were prepared containing 5 ml of LB, the required antibiotics and a colony from each LB plate. Following 4 hour incubation at 37 °C on a shaker, 1 starter culture was used to inoculate 0.5 L of LB which was again cultivated at 37 °C, whilst shaking, until an A_{600} of 0.6-0.8 was reached. Protein production was induced by adding IPTG (Promega) and the cultures were incubated overnight at 17 °C, shaking.

3.4.3. Harvesting the Recombinant Proteins

Cells were pelleted by centrifugation at 4,000 rpm for 20 minutes at 4 °C. The supernatant was removed and the remaining pellet was resuspended in 5 ml of 50 mM Tris-HCl pH 7.4, 100 mM NaCl and stored at -20 °C until use.

3.4.4. Small scale growth experiment

Optimal growth conditions were evaluated in a small scale growth trial. Small scale bacterial cultures (20 ml) were incubated at 37 °C until an A_{600} of 0.6-0.8 was obtained and then induced by the addition of IPTG. The cells were either maintained at 37 °C or transferred to 17 °C and kept shaking. The first set of cells at 17 °C and 37 °C was harvested after 2 hours (section 3.4.3). The two remaining cultures were left to grow overnight.

3.5. Protein Biochemistry Methods

3.5.1. Cell lysis

3.5.1.1. Cell lysis by detergent

Solutions

- ***Lysis Buffer***

Tris pH 8.3	50 mM
NaCl	150 mM

Triton X-100 0.1 %

Protein inhibitor cocktail without EDTA (Roche)

5Y° cells overproducing BACE1-MYC were transiently transfected with FLAG-RTN3 and cultured in 6-well-plates (section 3.2.6). The medium was aspirated and each well was washed with 1 ml PBS. The cells were lysed in 100 µl of lysis buffer, incubated on ice for 20 minutes and finally observed under a microscope to ensure complete lysis. The lysate was transferred into 1.5 ml micro-centrifuge tubes and pelleted by centrifugation for 30 minutes at 4 °C to remove cell residue. The supernatant containing the isolated protein was collected in 1.5 ml tubes.

Alternatively, for displaying BACE-MYC only, 5Y° cells were harvested as stated in section 3.2.4 and T-175 cell pellets were used for cell lysis.

3.5.1.2. Cell lysis by sonication

Recombinant bacteria grown and harvested as described in section 3.4.2 and 3.4.3 were lysed by sonication using a Sonics Vibracell Ultrasonic Processor. The samples were sonicated for 10 cycles of 30 seconds at 60 % amplitude and maintained on ice throughout. Lysed cells were pelleted by centrifugation (Beckman JA20 rotor) at 14,000 rpm at 4 °C for 20 minutes. The supernatant and pellet were collected in separate fractions. The pellet was resuspended in 5 ml of 50 mM Tris-HCl pH 7.4 and 100 mM NaCl.

3.5.2. Protein Purification

3.5.2.1. Individual Purification by MBP Affinity Column

Solutions

- ***Maltose Column Buffer***

  Tris-HCl pH 7.4 20 mM

  NaCl 200 mM

  EDTA 1 mM

- ***Maltose Column Elution Buffer***

Tris-HCl pH 7.4	20 mM
NaCl	200 mM
EDTA	1 mM
Maltose	10 mM

Methodology

In order to purify recombinant MBP-RTN3 HD individually a MBP affinity column was employed. Recombinant protein was produced in the *E.coli* strain *BL21-Codonplus(DE3)-RIL* (section 3.4.2), harvested (section 3.4.3) and lysed by sonication (section 3.5.1.2). Cell debris was pelleted by centrifugation at 14,000 rpm and 4 °C for 20 minutes. The supernatant containing MBP-tagged protein was applied to an amylose column (NEB) pre-equilibrated in 30 ml of maltose column buffer. The column was washed with 50 ml of maltose column buffer to remove non-specific protein and column-bound protein was eluted with elution buffer.

3.5.2.2. Individual Purification by GST Sepharose Column

Solutions

- ***Column Buffer (1x PBS) pH 7.4***

NaCl	140 mM
KCl	2.7 mM
Na_2HPO_4	10 mM
KH_2PO_4	1.8 mM

- ***Glutathione Elution Buffer***

Reduced Glutathione	10 mM
Tris-HCl pH 8.0	50 mM

Methodology

Recombinant proteins GST-BACE1 or GST were individually purified using a Glutathione Sepharose 4B column (GE Healthcare). Recombinant protein was

produced in the *E. coli* strain *BL21-Codonplus(DE3)-RIL* (section 3.4.2), harvested (section 3.4.3) and lysed by sonication (section 3.5.1.2). Cell debris was pelleted and the supernatant containing GST-tagged protein applied to the column pre-equilibrated in 30 ml of column buffer. The column was washed with 50 ml of buffer and resin-bound protein was eluted with glutathione elution buffer.

3.5.2.3. Dual-Purification of two proteins using a MBP Affinity Column

The aim of this method was to purify two interacting proteins using the same affinity column. Recombinant protein was produced (section 3.4.2), harvested (section 3.4.3) and lysed by sonication (section 3.5.1.2). Cell debris was pelleted and the supernatant containing MBP-tagged protein applied to an amylose column pre-equilibrated in 30 ml of maltose column buffer. The column was washed with 50 ml of maltose column buffer to remove non-specifically bound protein. The supernatant of the second recombinant protein was diluted 1:3 with column buffer and applied to the column. The column was washed with column buffer and any protein bound to the resin was retrieved by the addition of maltose column elution buffer. The elution fractions were collected in 1.5 ml micro-centrifuge tubes and either a Bradford Assay (section 3.5.4.1) or spectrophotometric analysis (section 3.5.4.2) was carried out to determine the concentration of purified protein.

3.5.3. Protein incubation

Protein was purified separately on a column with affinity for the specific tag (section 3.5.2). Protein concentration in the eluted fractions was measured using a Bradford Assay and adjusted for each sample to a 1:1 mixture ratio. Combinations of protein were incubated together for 12 hours at either 4 °C or 37 °C, whilst shaking.

3.5.4. Analysis of Protein Concentration

3.5.4.1. Bradford Assay

To calculate the concentration of protein the sample was diluted in dH_2O in a 96-well-plate. The following dilutions of 0.02, 0.05, 0.1 and 0.2 mg/ml BSA in dH_2O were used to delineate a standard curve. Bradford reagent (BioRad) was diluted 1:4 in dH_2O and 200 µl added to both standard and protein samples. Protein binding to the

dye stabilises its blue anionic form and the increase of absorbance at 595 nm is proportional to the quantity of bound dye and thus to the concentration of protein in the sample. To measure the protein concentration the plate was read at 595 nm on a Synergy HAT plate reader combined with KC4 Kineticalc for WindowsR software (both from BioTEK Instruments). The concentration was calculated in mg/ml.

3.5.4.2. Spectrophotometric analysis using Nanodrop

To calculate the concentration of purified protein in the elution fractions the Thermo Scientific NanoDrop™ 1000 Spectrophotometer in combination with the Nanodrop 1000 3.7.1 software was used. An aliquot of 1.2 µl of sample was applied and the absorption rate (A) at 280 nm was measured. The accurate protein concentration (c) in mg/ml was calculated according to equation 3.2. The extinction coefficient (ε = 70820) was determined using Expasy (http://www.expasy.org) under specification of the entire amino acid sequence (Figure 4.10).

$$Protein\ concentration\ (mg/ml) = \frac{(A_{280} \times \varepsilon)}{Molecular\ Weight} \qquad (3.2)$$

3.6. Gel Electrophoresis and Western Blotting Analysis

3.6.1. SDS-Polyacrylamide Gel Electrophoresis

Solutions

- ***1x SDS Running buffer***

Tris Base	25 mM
Glycine	200 mM
SDS	1 %

- ***SDS Sample Buffer (Laemmli Buffer)***

Tris-HCl pH 6.8	60 mM
Glycerol	10 %
SDS	2 %
β-mercaptoethanol	100 mM
Bromophenol Blue	1 %

Resolving Gel 12 % (ml)		**Stacking Gel 5 % (ml)**	
3.3	H_2O	1.4	H_2O
4.0	Acrylamide mix 30 %	0.33	Acrylamide mix 30 %
2.5	1.5 M Tris (pH 8.8)	0.25	1.0 M Tris (pH 6.8)
0.1	SDS 10 %	0.02	SDS 10 %
0.1	Ammonium persulfate (10 %)	0.02	Ammonium persulfate (10 %)
0.004	TEMED	0.002	TEMED

Table 3.9. *Solutions for a 12 % SDS-PAGE Gel (according to protocols in Molecular Cloning, Sambrook et al.)*

Methodology

A 12 % SDS gel was used throughout in order to achieve optimal protein separation. Benchmark™ Protein Ladder, MagicMark™ XP Western Standard and SeeBlue™ Pre-Stained Standard (Invitrogen) were used as protein markers with standard molecular weights as a comparison to the actual protein (Figure 3.2). Samples were diluted with dH_2O and SDS sample buffer to obtain a final protein concentration of 1 µg/µl. The samples were boiled for 10 minutes to further denature the protein. The gel was inserted into the gel tank (XCell *SureLock*™ Mini-Cell, Invitrogen), submerged in 1x SDS running buffer and 10 µl aliquots of sample were loaded onto the gel. A 200 Volt electric current was applied for 1 hour.

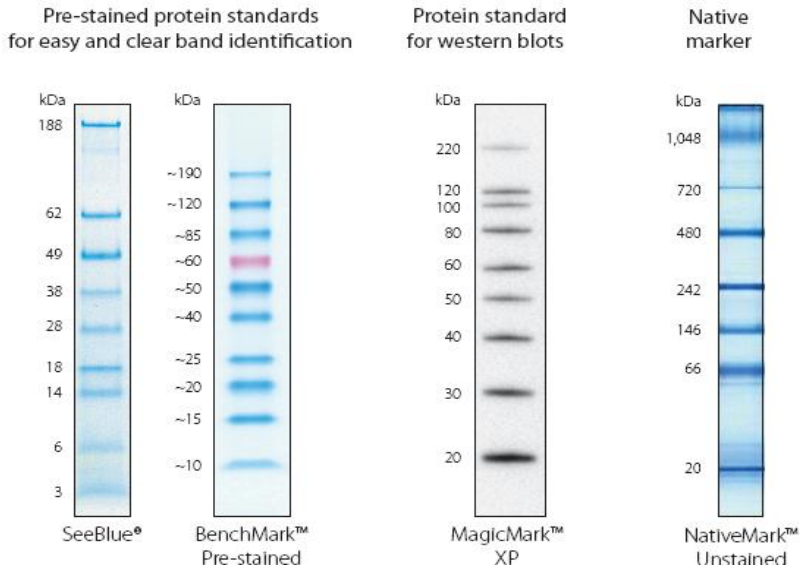

Figure 3.2. *Invitrogen Markers used in this study.*

3.6.2. Native Polyacrylamide Gel Electrophoresis

Solutions

- ***1x Native Running buffer***

  Trizma ® base 25 mM

  Glycine 200 mM

- ***Native Sample Buffer***

  0.5M Tris-HCl pH 6.8 60 mM

  Glycerol 10 %

  Bromophenol Blue 1 %

Native resolving Gel 8 % (ml)		**Native stacking Gel 5 % (ml)**	
4.7	H_2O	1.42	H_2O
2.7	Acrylamide mix 30 %	0.33	Acrylamide mix 30 %
2.5	1.5 M Tris (pH 8.8)	0.25	1.0 M Tris (pH 6.8)
0.1	Ammonium persulfate (10 %)	0.02	Ammonium persulfate (10 %)
0.006	TEMED	0.002	TEMED

Table 3.10. *Solutions for a 8 % native PAGE-Gel (according to protocols in Molecular Cloning, Sambrook et al.)*

All samples were diluted with native sample buffer to a final concentration of 10 µg/ml and the gel was submerged in native running buffer. The samples were loaded on to the gel and a native marker (NativeMark, Invitrogen) was added as a reference. During the 2 hours run at 100 Volts the gel tank was placed inside an ice-box to prevent it from overheating.

3.6.3. Coomassie stain

Solutions

- ***Coomassie Blue Stain***

Brilliant Blue	0.25 %
Methanol	50 %
dH_2O	50 %
Glacial acetic acid	10 %

Following Gel-Electrophoresis the native or SDS gel was placed inside a box, submerged in coomassie stain and left on a rocker for 30 minutes. The gel was rinsed carefully with distilled water and heated in a microwave for 10 minutes. Heating was repeated until the desired resolution was achieved. The destained gel was dried using the DryEase® gel drying system from Invitrogen and stored between two sheets of cellophane.

3.6.4. Western blotting

Solutions

- ***Transfer buffer***

Tris-HCl pH 8.0	25 mM
Glycine	192 mM
Methanol	2 %

- ***PBST***

NaCl	140 mM
KCl	3 mM
Na_2HPO_4	10 mM
KH_2PO_4	2 mM
Tween 20	0.05 %

- ***Blocking Solution***

  5 % dry non-fat milk powder in PBST

Methodology

After completion of either SDS or Native PAGE the stacking gel was removed and a nitrocellulose membrane was placed on top of the gel with filter paper and blotting pads around it (Figure 3.3). The whole "sandwich" was placed inside a transfer cell (XCell®), transfer buffer was added and a constant current of 30 Volts was applied for 1 hour causing the proteins to move from the gel onto the membrane. Once the transfer was finished the membranes were submerged in blocking solution and left shaking for 1 hour at room temperature. Three repeats of five minute washing steps in PBST were completed and the primary antibody (Table 3.11) was incubated for 1 hour, followed by another three 5 minute washing steps in PBST. The membrane was exposed to the appropriate secondary antibody (Table 3.12), conjugated to the reporter enzyme horseradish-peroxidase. Three additional 5 minute washing steps in PBST followed. In the dark the chemiluminiscent agent ECL Plus™ (GE Healthcare) was applied to the membrane, producing luminescence in proportion to the amount of protein bound. The signal was detected using a sheet of photographic film and exposing for 15-30 minutes. The film was developed and fixed (Kodak) to obtain suitable resolution.

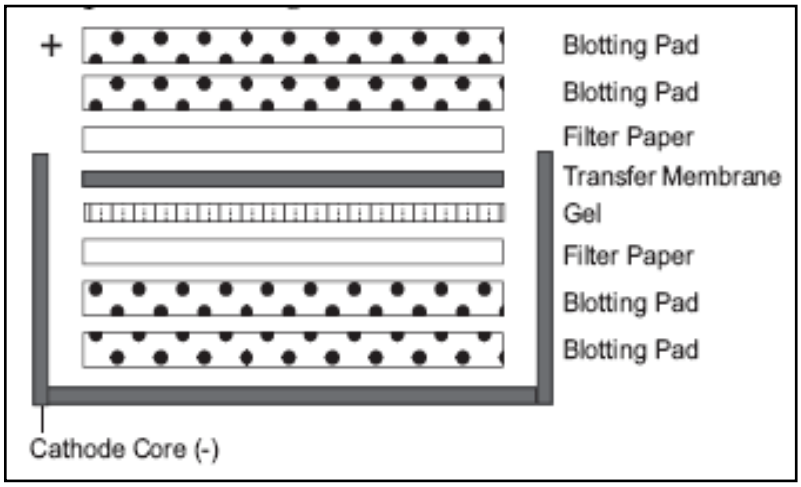

Figure 3.3. *Setup for a western blot transfer using XCell II™ Blot Module (Invitrogen). Taken from the XCell manual.*

Antibody	Host	Dilution	Recognition site	Source
MAB5308	Mouse mAB	1/1000	Human BACE	Millipore
α-MBP	Mouse mAB	1/500	MBP derived of *mal*E gene of *E.coli*	Invitrogen
PC478	Rabbit pAB	1/1000	aa 44-59 of human BACE	Calbiochem
9E10	Mouse mAB	1/1000	aa 408-432 human c-Myc	Abcam
α-FLAG	Mouse mAB	1/1000	FLAG	Sigma-Aldrich

Table 3.11. *Primary antibodies used in this study.*

Antibody	Host	Dilution	Conjugate	Source
Anti-Mouse	Goat	1/10000	H&L Chain Specific Peroxidase	Calbiochem
Anti-Rabbit	Donkey	1/10000	HRP-Linked Whole Antibody	GE Healthcare

Table 3.12. *Secondary antibodies used in this study.* HRP*: Horseradish Peroxidase,* H&L*: heavy and light chain.*

CHAPTER 4

RESULTS

4.1. Introduction

Alzheimer's disease is a neurodegenerative disorder where cause and progression are still not well understood. Research indicates that the disease is associated with the accumulation of misfolded β-amyloid, a small peptide, 39–43 amino acids in length, which originates from a larger precursor protein (APP). Inhibiting the activity of the β-amyloid converting enzyme 1 (BACE1) decreases the production of β-amyloid. Membrane bound reticulon (RTN) family proteins interact with BACE1 and negatively modulate BACE1 activity through preventing access of BACE1 to its cellular APP substrate (He *et al.*, 2004). This study focused on RTN3, which is largely expressed in neurons and therefore a potential candidate for inhibiting BACE1. The general aim of this study was to reconstitute binding between BACE1 and RTN3.

4.2. Expression of RTN3 in cell cultures

The first approach to investigate the interaction between RTN3 and BACE1 was to replicate the results observed by He *et al.* (2004). In these experiments a SH-SY5Y derived cell line (5Y°) was used, which stably expresses C-terminally MYC-tagged BACE1 (Dr Ruth Rose, Kings College, London).

4.2.1. Lysis of BACE1-MYC cells

In a preliminary experiment cell lysis conditions were evaluated. Since the detergents were not disclosed in the original paper describing the interaction (He *et al*., 2004), different types and concentrations of commonly used lysis buffers were assessed in the efficacy to extract membrane-bound BACE1-MYC protein. A solution of 0.1 % Triton X-100 buffer proved to be the most efficient in the lysis of BACE1-MYC over-

producing 5Y° cells and allowed a good resolution of BACE1-MYC by western blot (Figure 4.1).

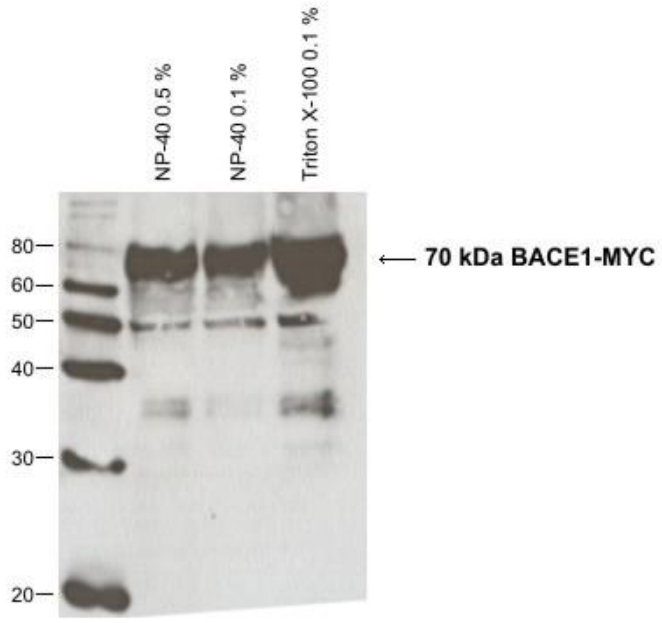

Figure 4.1. Different concentrations of lysis buffer were assessed. *Cells were lysed with 0.1% NP-40, 0.5% NP-40 and 0.1% Triton X-100. Triton X-100 induced the generation of smaller micelles and therefore liberated clearly more BACE1. Antibody: MAB5308*

This way the efficiency of 5Y° cells in over-producing BACE1-MYC was verified and successful liberation of the integral membrane protein by the employed detergent was confirmed.

4.2.2. Transfection of BACE1-MYC cells with pFLAG-RTN3

BACE1-MYC-5Y° cells were transiently transfected with full length FLAG-tagged *RTN3*. The pFLAG-*RTN3*-CMV-6c template was received from Dr Mitsuo Tagaya, Department of Pharmacy & Life Science at Tokyo University. Cells were allowed to grow for 3 days at 37 °C with 95 % air and 5 % CO_2. For all further experiments a preparation of crude cell lysates was used. Cell lysis was carried out in 0.1 % Triton X-100 buffer and a Bradford assay was done to calculate and adjust the concentration of protein (1 µg/µl). The lysates were directly applied to SDS-PAGE. Results were observed by Western Blot, using Anti-FLAG and Anti-BACE (MAB5308) antibodies. BACE1-MYC showed a good resolution on the gel (Figure 4.2). However, no FLAG-RTN3 was observed in transfected cells (data not shown).

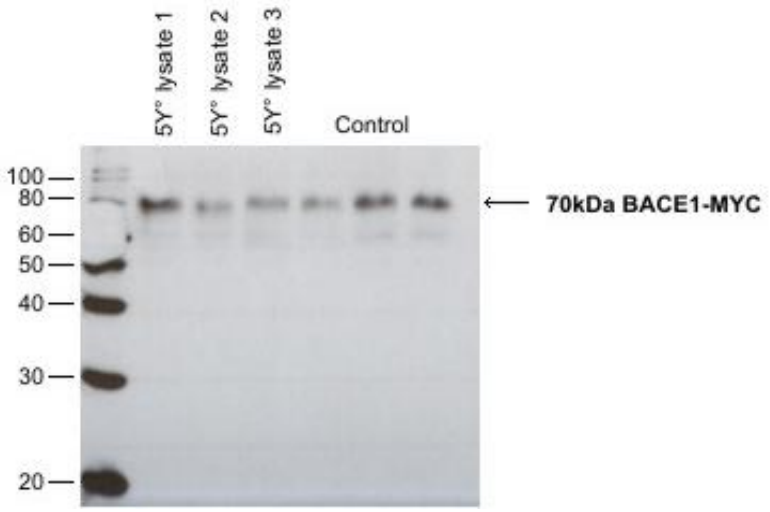

Figure 4.2. **Western blot for BACE1-MYC in 5Y° cells.** *BACE1-MYC is represented by the prominent band around 70kDa. Transfection was performed in triplicate. Control denotes 5Y° cells without transfection. Antibody: MAB5308.*

Attempts to optimise transfection conditions were implemented but to no avail. For this reason an alternative method was employed to investigate BACE1 and RTN3 interaction.

4.3. Recombinant production of RTN3 and BACE1

4.3.1. General approach

An alternative approach to investigate the interaction between RTN3 and BACE1 involved using recombinantly produced RTN3 and BACE1. The domain encoding the proposed binding site of RTN3 (section 4.3.2) was cloned into the expression vector pMal-c2x, which is designed to generate a MBP fusion protein. The *mal*E gene on this vector is deleted for the signal sequence, leaving the produced fusion protein to remain in the cytoplasm. Cells therefore need to be lysed (section 3.5.1.2) and then purified (section 3.5.2). The introduction of a MBP tag facilitated one-step affinity protein purification and allowed quick and efficient isolation of RTN3. Figure 4.3 illustrates a more detailed schematic of the process.

Advantages and limitations of a recombinant approach will be discussed in more detail in chapter 5.

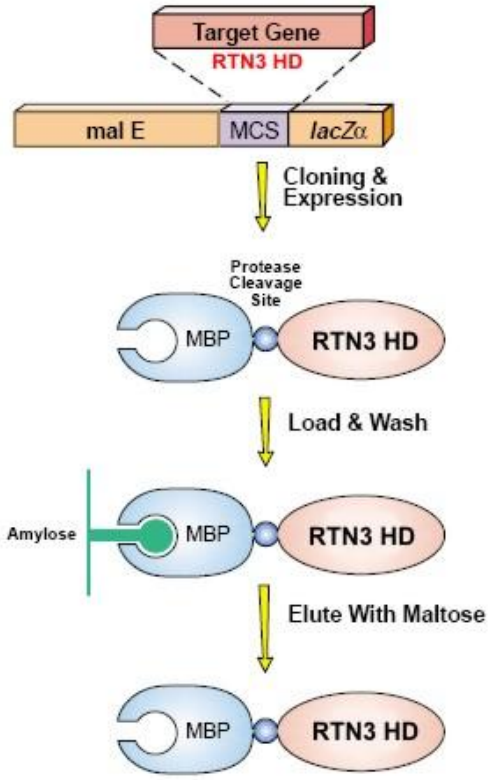

Figure 4.3. MBP fusion protein. *The cloned gene is inserted into a restriction site of the vector polylinker, in the same translational reading frame as the malE gene, which encodes maltose-binding protein (MBP). This results in the expression of an MBP-fusion protein. The technique uses the strong P_{tac} promoter and the translation initiation signals of MBP to express large amounts of the fusion protein. The fusion protein is purified using an amylose column. (pMAL™ Protein Fusion and Purification System, NEB)*

4.3.2. Identification of the RTN3 Homology Domain

In order to reconstitute interaction between RTN3 and BACE1 it was decided to use a RTN3 variant containing only the region that was proposed to mediate binding. RTN proteins are characterised as a group of membrane bound proteins that share a highly conserved C-terminal Reticulon Homology Domain. The interaction of BACE1 with all four RTN members implies that this domain may mediate binding of RTNs to BACE1 (*He et al., 2004*). It was previously shown that a completely conserved QID amino acid triplet within the C-terminal tail of RTNs is critical for the interaction (*He et al., 2006*). For the following studies a truncated RTN3, termed RTN3 Homology Domain (RTN3 HD), was designed, consisting merely of the last C-terminal 40 amino acids including the anticipated binding site (QID) but lacking predicted loop and transmembrane regions.

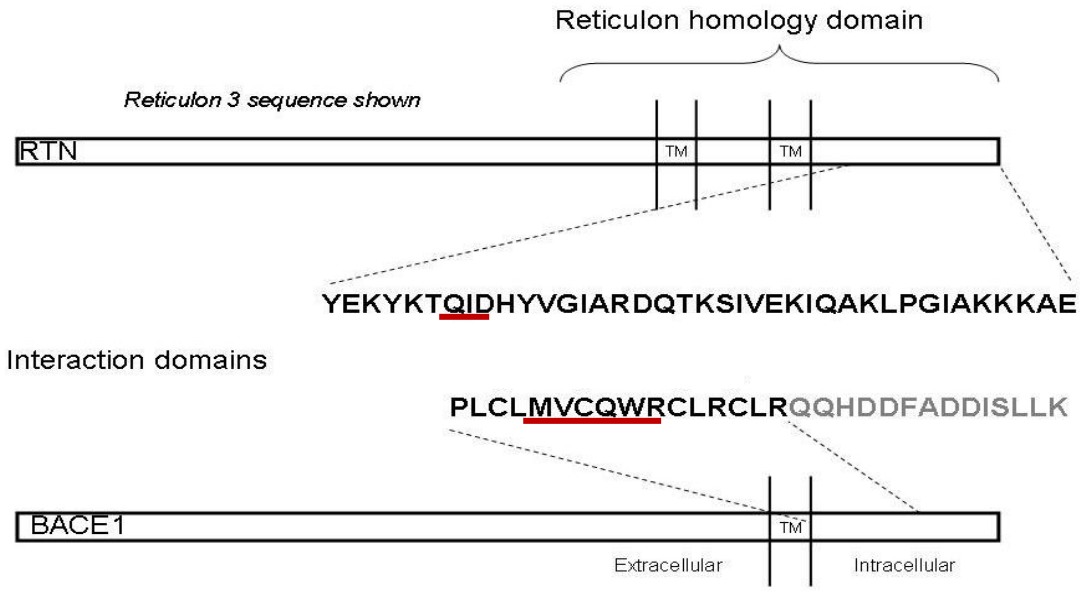

Figure 4.4. *BACE1-RTN3 interaction domains*. *The proposed binding sites are underlined in **red**. In this study both BACE1 and RTN3 were truncated to the specified amino acid sequence. (C. Dingwall, King's College London)*

4.3.3. Cloning of RTN3 HD

Primers were designed to replicate the C-terminal homology domain of RTN3 which will be referred to as RTN3 HD from here on. Additionally the restriction sites for *Bam*HI and *Hind*III were incorporated into the sequence to allow the gene to be inserted into pMal-c2x. The amplification of RTN3 HD is shown on the diagram below (Figure 4.5).

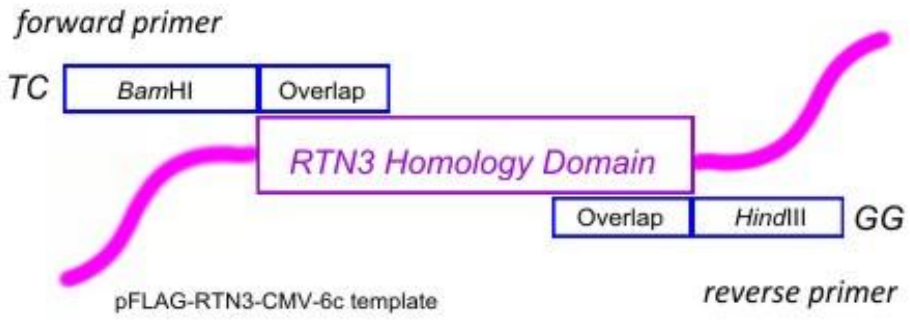

Figure 4.5. Amplification of the Homology Domain. *The primers BamHI and HindIII were incorporated into the sequence.*

Polymerase Chain Reaction (PCR) was used to amplify the selected DNA sequence. DNA fragments were analysed by agarose gel electrophoresis (Figure 4.6),

extracted, digested with the designated restriction enzymes and ligated into the pMal-c2x expression vector. JM109 cells were transformed with the ligation product and screened by colony PCR (data not shown) to identify colonies that carried the insert. Four colonies containing the insert were picked and a miniprep was prepared. An analytical restriction digest confirmed the presence of the insert (Figure 4.7) and isolated DNA was sent in for sequencing (Figure 4.8). The result determined the nucleotides of the template DNA to be in alignment with the predicted sequence (Figure 4.9).

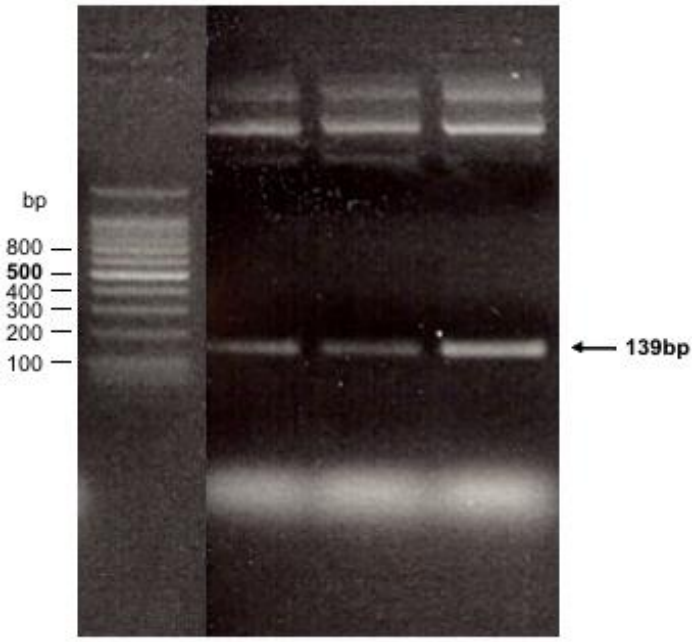

Figure 4.6. PCR

RTN3 HD DNA was amplified in triplicate and analysed by agarose gel electrophoresis. Bands appearing at appropriate size (139 bp) were excised, extracted, digested and ligated into the vector pMal-c2x. The ligation product was introduced into JM109 competent cells. Commercial 100bp marker used: see page 20.

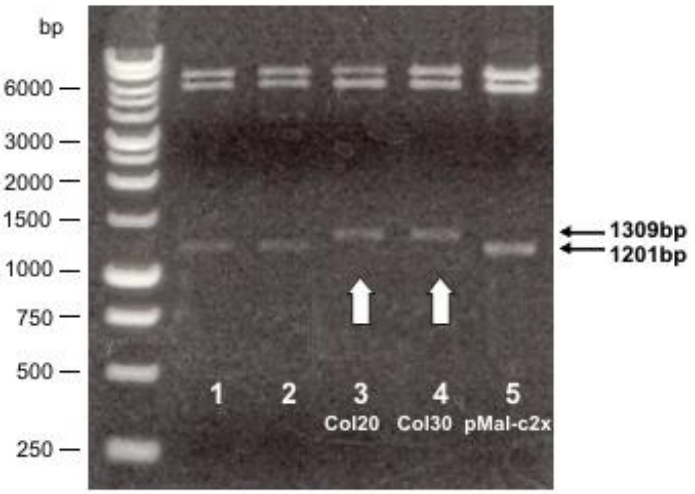

Figure 4.7. Restriction digest

An analytical digest with 2 different restriction enzymes was performed to check if DNA strands were ligated correctly. Resulting constructs were compared to the empty vector pMal-c2x (5). The low MW bands of construct 3 & 4 show at 1309 bp, considerably higher than the vector's band (1201 bp) which suggests they carry the insert. Colony 20 and 30 were sent in for sequencing at GATC Biotech (Konstanz, Germany).

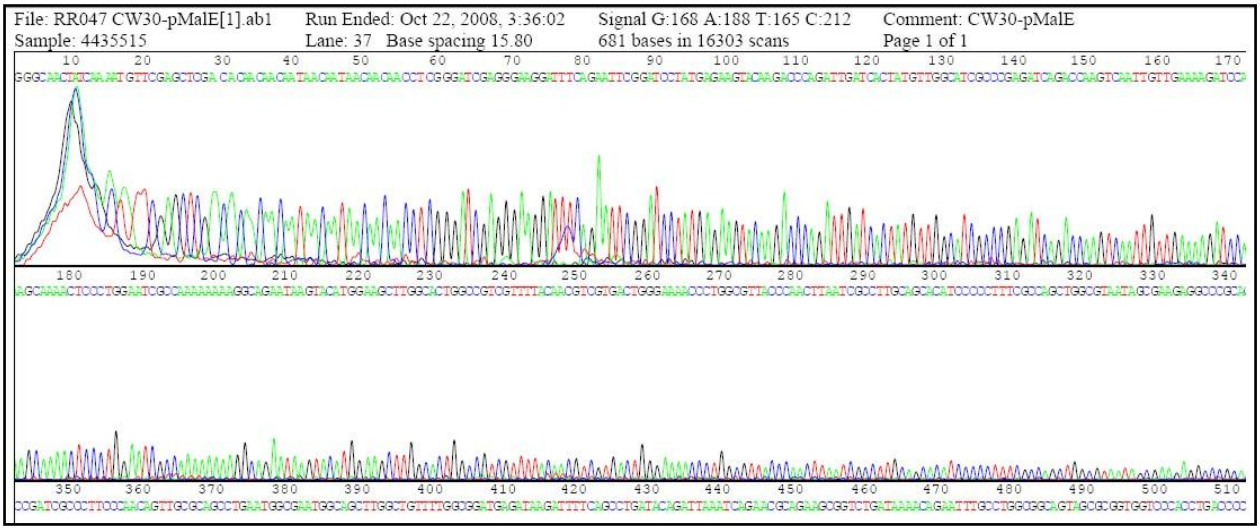

Figure 4.8. Sequencing results *from GATC (Konstanz, Germany). Colony 30 was selected as it had the correct sequence alignment.*

RTN3 HD was successfully cloned into the vector pMal-c2x.

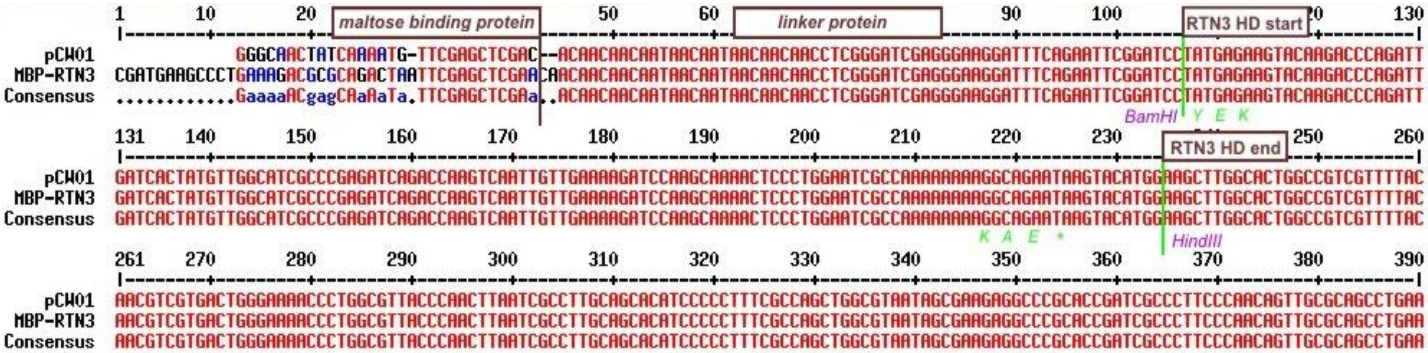

Figure 4.9. MBP-RTN3 HD sequence alignment. *Red marks aligned base pair; blue, different base pair; dots indicate deletions. Alignment was verified using MultAlin (http://bioinfo.genotoul.fr/multalin/ multalin.html).*

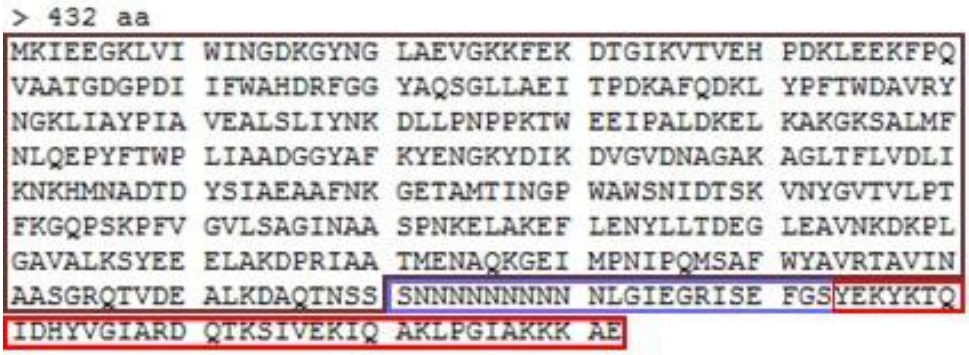

Figure 4.10. Translated amino acid sequence of sequenced pCW01 expression vector. *The frames mark maltose binding protein, linker protein and RTN3 HD. Molecular weight according to Expasy (http://www.expasy.org): 47574.8 Da.*

4.3.4. Protein Production

Protein production was assessed by a small scale trial (20 ml). Competent *BL21-Codonplus(DE3)-RIL* cells were transformed with the pMal-c2x-RTN3 HD expression vector, containing the verified sequence (pCW01), and colonies were selected on ampicillin and chloramphenicol. Cells were grown at 37 °C until an A_{600} of 0.6-0.8 was obtained. Protein production was induced by the addition of IPTG. The cells were either maintained at 37 °C or transferred to 17 °C and were kept shaking. After 2 hours, one flask grown at 37 °C and one at 17 °C were harvested by centrifugation. All remaining cultures were left to grow overnight. The cells were pelleted and resuspended in 50 mM Tris pH7.4, 100 mM NaCl. Cells were lysed by sonication and pelleted by centrifugation. All samples were run on a Western Blot to confirm the presence of MBP-RTN3 HD (Figure 4.11).

Nr	Temp °C	Induction	Vol
1	37	o/n	20
2	37	2h	20
3	17	2h	20
4	17	o/n	20

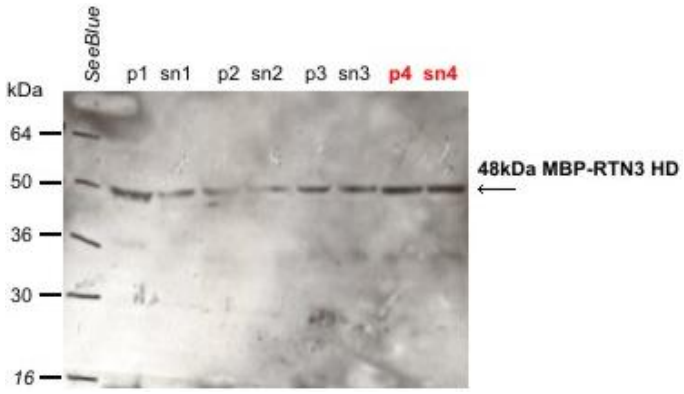

Figure 4.11. Induction trial. *Protein production was induced with IPTG, cells were grown at 37°C or 17°C, samples were taken after 2 hours and 12 hours (o/n).* P*: post lysis pellet resuspended in column buffer,* Sn*: post lysis supernatant. Marker: SeeBlue®. AB: α-MBP.*

MBP-RTN3 HD bands appeared at the expected size of 48 kDa. Overnight protein production at 17 °C generated the greatest yield (Figure 4.11); therefore all further studies were carried out under these conditions. It was also observed that following cell lysis a significant concentration of protein still remained in the pellet.

4.3.5. Protein Purification

Purification of MBP-RTN3 HD was accomplished using a one-step affinity purification column that allowed fast, efficient and non-denaturing protein extraction directly from microbial cultures. The plasmid carrying MBP-*RTN3* HD was introduced into the expression strain and recombinant protein was produced in a large scale induction culture (0.5 litres), growing at 17 °C overnight as described above (section 4.3.4). The cells were lysed by sonication, pelleted by centrifugation and the supernatant, containing the soluble protein, was applied to an amylose column with high affinity for the MBP fusion protein. The acquired fractions were stored and analysed by SDS-PAGE to evaluate protein purification and expression levels. Results are shown in Figure 4.12.

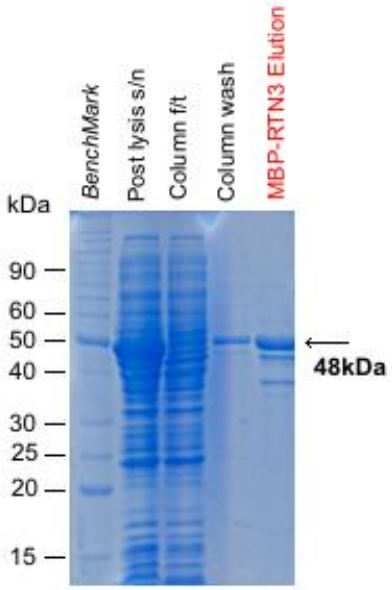

Figure 4.12. SDS-PAGE analysis of affinity purification of MBP-RTN3 HD. *See table 4.1 for sample descriptions. Elution fractions are marked red, marker in italics. 12% SDS gel.*

The elution fraction containing the purified MBP-tagged RTN3 HD protein showed a sharp band at approximately 48 kDa which is consistent with the expected size. A weaker band was also detected at 38 kDa, possibly being evidence of protein fragmentation as it was consistently visible in 3 purification repeats under the stated conditions (data not shown).

Regarding these outcomes the presented method was considered an efficient and reproducible way to produce recombinant RTN3 HD at a substantial yield.

4.3.6. Potential dimerisation of MBP-RTN3 HD

In a separate experiment purified elution fractions of MBP-RTN3 HD were run on native PAGE to study the generation of complexes and oligomers. These gels indicated the presence of an additional band at approximately 90 kDa (Figure 4.13), possibly representing a dimer. MBP-RTN3 HD dimers were calculated to appear at about 95 kDa. Bands corresponding to that size were visible throughout on all native gels (section 4.3.9).

These findings are in accordance with observations made by *He et al.*, 2006, who identified RTN3 homo- and heterodimerisation. Additional contaminating bands were detected at approximately 25 and 30 kDa. Surprisingly, no band was observed at 48 kDa, matching the calculated size of the original MBP-RTN3 HD monomer. As it appears these monomers instantly aggregate to form larger complexes that can only be separated by strong denaturing conditions.

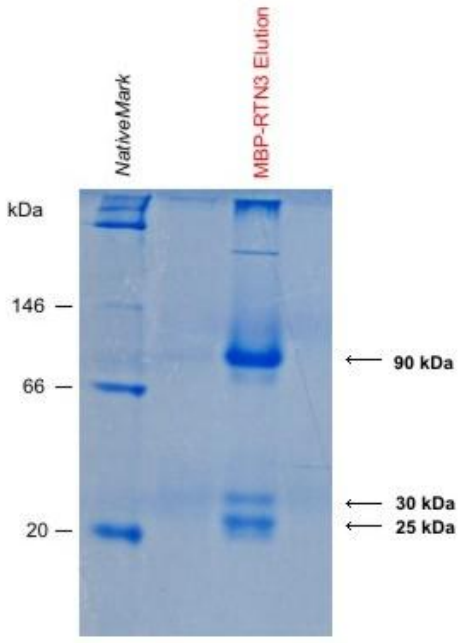

Figure 4.13. Native-PAGE analysis of individual purification of MBP-RTN3 HD. *Run with NativeMark. 8% native gel.*

As it was not entirely clear how these complexes evolve, several investigative trials were conducted to characterise the interaction. The result of this analysis can be found in section 4.3.8.

4.3.7. Dual-Purification of MBP-RTN3 HD and GST-BACE1

Based on the common principles of Immunoprecipitation and Tandem Affinity Purification (*Puig et al., 2001*) a new method was developed to combine both protein purification and binding studies of RTN3 HD and BACE1. Immunoprecipitation uses protein A or G beads coated with an antibody that is specific for a known motif to isolate it from a crude lysate. In contrast, Tandem Affinity Purification involves the creation of a fusion protein with a TAP-tag consisting of Protein A that binds tightly to IgG and calmodulin binding peptide. The protein of interest is then retrieved with two affinity columns binding to each moiety.

This study adopted the technique of introducing a specific tag to retrieve the protein on an affinity column, in this case MBP-RTN3 HD. The second protein and potential binding-partner, GST-BACE1 (vector designed by Dr B Angelleti), carried a different tag to prevent artefactual binding. To simplify matters both proteins were applied to the same column and elution fractions were screened for both proteins, which would indicate successful protein-protein interaction.

Gel sample	**Description**
Cell pellet	Post lysis and centrifugation cell pellet resuspended in column buffer.
Post lysis s/n	Post lysis and centrifugation supernatant.
Column f/t	Lysis supernatant column flow through.
Column wash	Post binding column washed with 50 ml of column buffer.
Elution	Most concentrated fraction eluted from the column.
Dual eluate	Most concentrated elution fraction after dual purification.
MBP-RTN3	MBP-tagged homology domain of RTN3.

Table 4.1. *Caption of all samples used for SDS-PAGE and Western Blot analysis of the dual purification.*

The crude cell extracts of freshly produced MBP-tagged RTN3 HD were applied to an amylose column allowing the fusion protein to bind directly to the polysaccharide resin whilst all other bacterial proteins were removed by washing under gravity flow. The first protein, MBP-RTN3 HD, was now held in solid phase by MBP and the second lysate, containing GST-BACE1 was applied in a liquid phase. The fusion

proteins were given time for their C-terminal partners to interact, then the column was washed again. The protein-complex was eluted from the amylose resin with maltose. All fractions were collected and run on SDS- and native PAGE. The results were observed by coomassie staining (Figures 4.14, 4.16) and Western Blot (Figure 4.15).

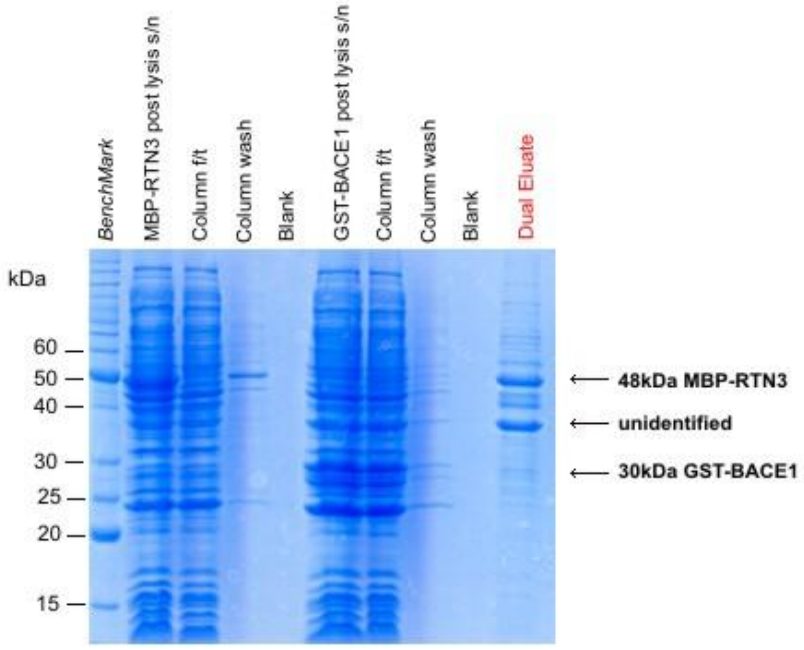

Figure 4.14. SDS-PAGE analysis of dual purification of MBP-RTN3 HD and GST-BACE1. *Table 4.1 for sample descriptions. Elution fractions are marked red, marker in italics.*

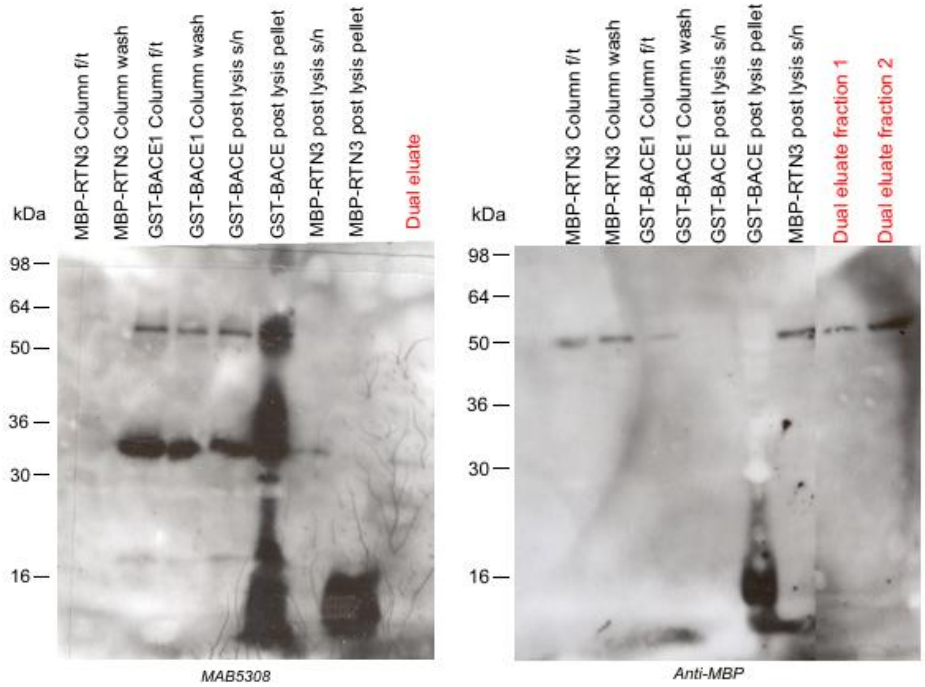

Figure 4.15. Western blot of dual purification. *MBP-RTN3 HD was clearly detected by the α-MBP antibody in both elution fractions at 48kDa. GST-BACE1 was not observed in the dual eluate despite being visible in the flow-through and washing fractions.*

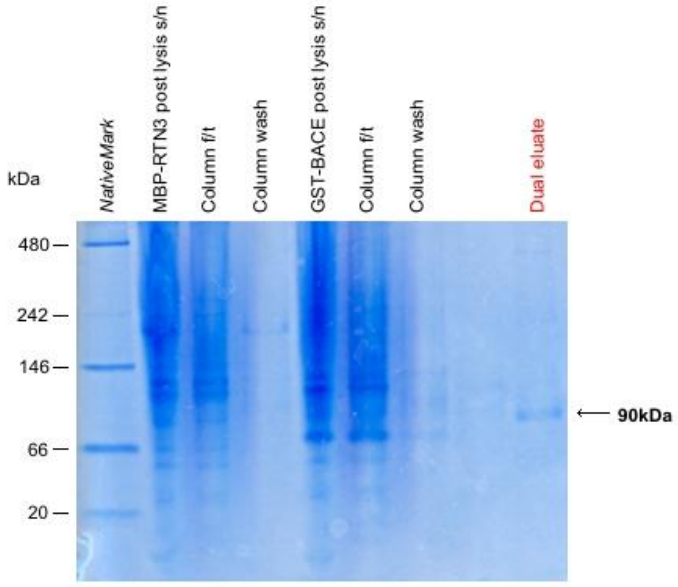

Figure 4.16. Native PAGE analysis of dual purification. *Run with NativeMark. See table 4.1 for sample descriptions. 8% native gel.*

In the elution fraction there is no distinct band detectable at 30 kDa on the denaturing SDS gel (Figure 4.14) although GST-BACE1 is clearly visible in the post-lysis supernatant and the column flow-through. This result was once more confirmed by Western Blot using specific antibodies against BACE1 and MBP (Figure 4.15). It is therefore evident that MBP-RTN3 HD and GST-BACE1 were not eluted together as a consequence of interaction. The product is contaminated with several other bands including the previously observed fragment at 38 kDa (Figure 4.12).

A non-denaturing native gel (Figure 4.16) showed a high molecular weight band at approximately 90 kDa that could indicate successful protein-protein interaction. However, previous studies have confirmed the presence of a potential MBP-RTN3 HD dimer at that particular size (Figure 4.13). Along with the inconclusive result of the SDS-PAGE and Western Blot this does not confirm binding of RTN3 to BACE1. Consequently an alternative and more direct methodology was employed.

4.3.8. Individual purification and incubation

To enhance the possibility of both proteins interacting with each other, MBP-RTN3 HD, GST-BACE1 and a negative control of GST were purified individually on an affinity column specific for the fusion protein (Figure 4.17). All eluted fractions containing purified protein were incubated together in a series of experiments under

various conditions. Two different combinations of protein were maintained for 12 hours at either 37 °C or 4 °C and then run on SDS (data not shown) and native PAGE (Figure 4.18).

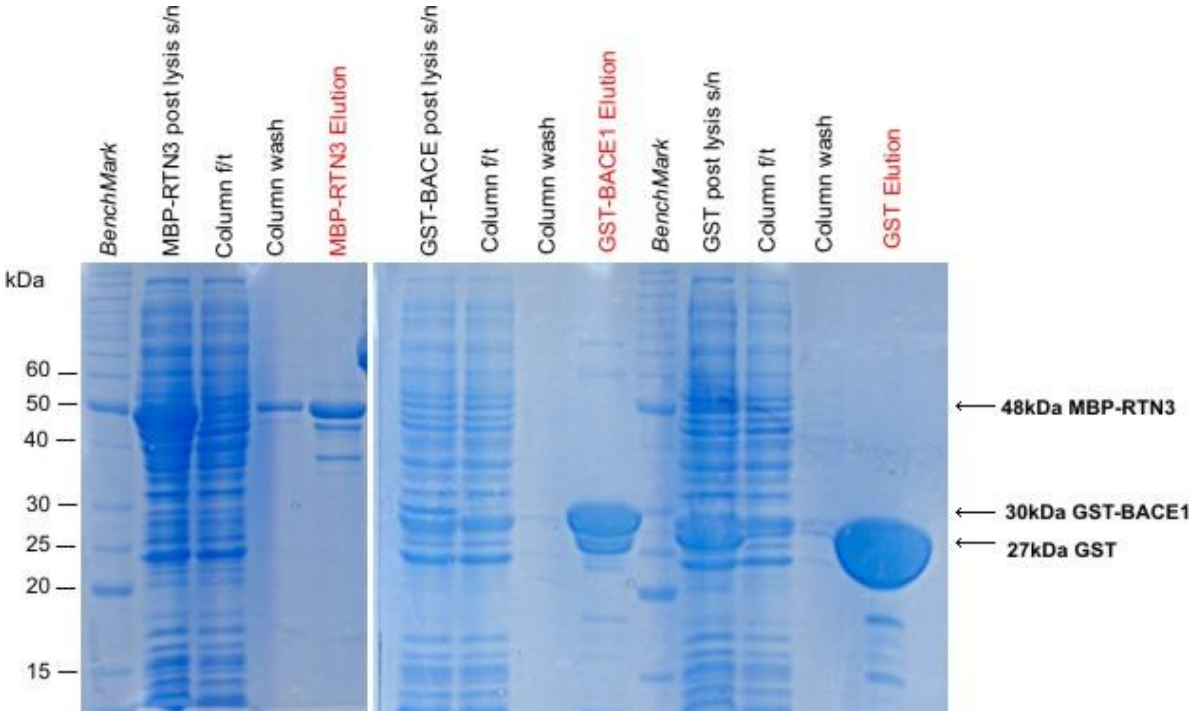

Figure 4.17. SDS-PAGE analysis of individual purifications for MBP-RTN3 HD, GST-BACE1 and GST. *Run with BenchMark. See table 4.1 for sample descriptions.*

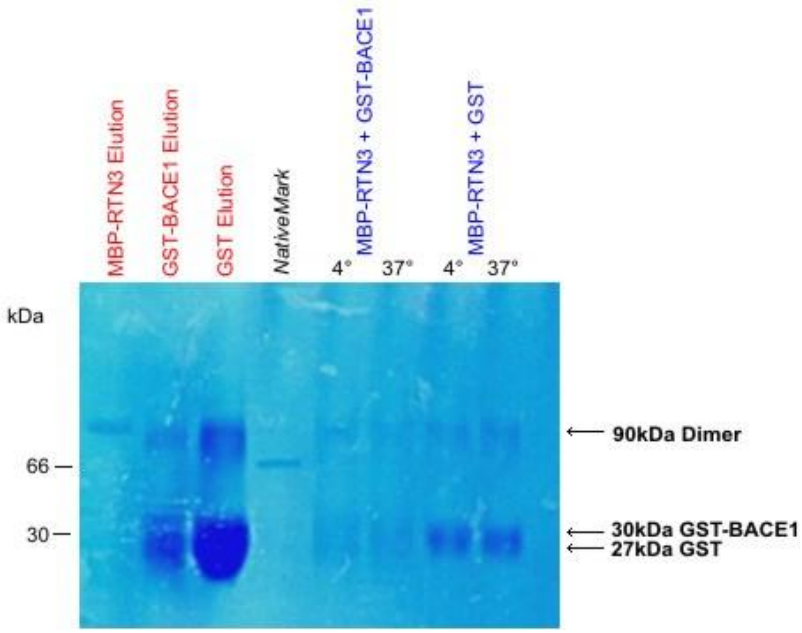

Figure 4.18. Native-PAGE analysis of individual purifications for MBP-RTN3 HD, GST-BACE1 and GST. *Run with NativeMark. Purified proteins from the elution fractions* (red) *were incubated (blue) overnight at 37°C with gentle agitation at a 1:1 ratio. 8% native gel.*

All SDS gels run with purified samples show sufficient levels of protein production for the incubation studies (Figure 4.17). Hence an adequate concentration of protein was provided for all further binding assays (10 µg/ 10 µl). For the investigation of potential protein-protein interaction a non-denaturing native gel was used. If native PAGE is carried out near neutral pH to avoid acid or alkaline denaturation, it can be used to study conformation, self-association or aggregation, and the binding of other proteins or compounds.

Elution fractions were incubated in two combinations (Figure 4.18) and run on the native gel. Higher molecular weight bands at approximately 90 kDa were identified in the incubation samples corresponding to those observed in the elution fractions. As discussed in section 4.3.6 this could be evidence for oligomerisation of MBP-RTN3 HD whilst it seems very unlikely that protein binding occurred during the incubation period.

4.3.9. Analysis of the interaction

To further probe the interaction, all proteins were purified separately under a variety of conditions, incubated and run on a native gel to be confident of complex formation. Samples were incubated for either one hour (data not shown) or overnight, at 4 °C and 37 °C.

High salt conditions

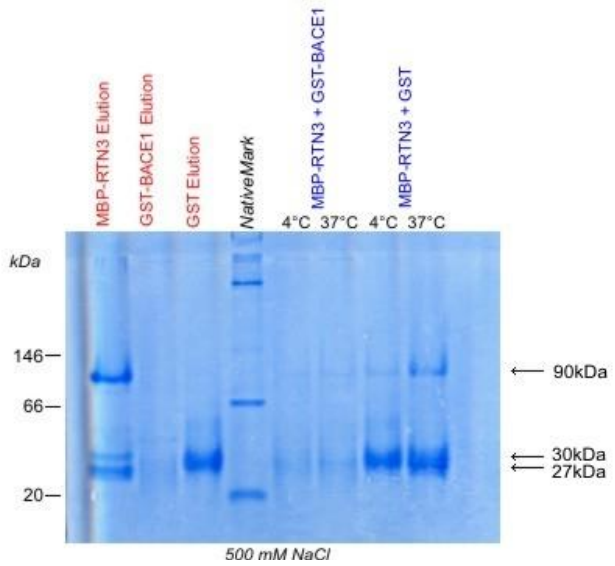

Figure 4.19. Native-PAGE of individual purifications *of MBP-RTN3 HD, GST-BACE1 and GST with addition of 500 mM NaCl to all buffers. Overnight incubation at 4 °C & 37 °C (blue).*

In general, the addition of salt disrupts protein-protein interactions on the basis of charge. Increasing the salt concentration reduces the strength of ionic binding by providing competing ions for the charged residues of a protein. In this study the concentration of NaCl in all purification buffers was increased to 500 mM in order to observe alterations in protein structures caused by ionic charges. High salt conditions severely diminished the concentration of purified protein in the elution fractions. In particular GST-BACE1 was affected with protein levels being below the threshold of detection. This observation and the general loss of intensity in most bands are largely due to precipitation. High-salt conditions are known to promote the interaction of surface hydrophobic regions on proteins, inducing the formation of aggregates that separate from the water (*Marshak, 1996*). However, the grade of multimerisation observed by native PAGE (Figure 4.19) resembled those seen under the standard purification conditions (Figure 4.18).

Low salt conditions

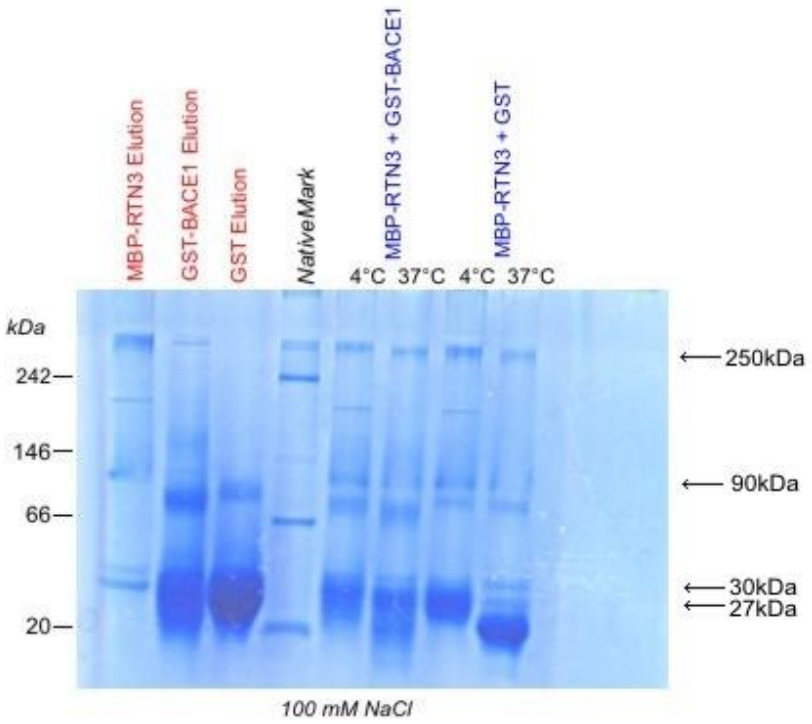

Figure 4.20. Native-PAGE of individual purifications *of MBP-RTN3 HD, GST-BACE1 and GST with addition of 100 mM NaCl to all buffers. Overnight incubation at 4 °C & 37 °C (blue).*

Low salt conditions or a reduced number of free ions in solution are expected to enhance the strength of ionic binding among the charged groups on the surface of a protein. In this study, a significant increase in multimerisation in MBP-RTN3 HD and

GST-BACE1 samples was induced. In contrast to high salt purification conditions, a GST multimer appeared also, visible in the GST elution fraction as well as in GST-BACE1 samples.

MBP-RTN3 HD showed slightly less multimerisation when incubated overnight at 37°C suggesting temperature-dependent degradation of higher molecular weight complexes (Figure 4.20).

There was no evidence for binding between incubated samples of GST-BACE1 and MBP-RTN3 HD induced by low salt purification conditions. Individual proteins tended to interact with themselves and oligomerise more readily during purification. However, this did not have any effect on heterogenous interaction during incubation.

Strong reducing conditions (DTT)

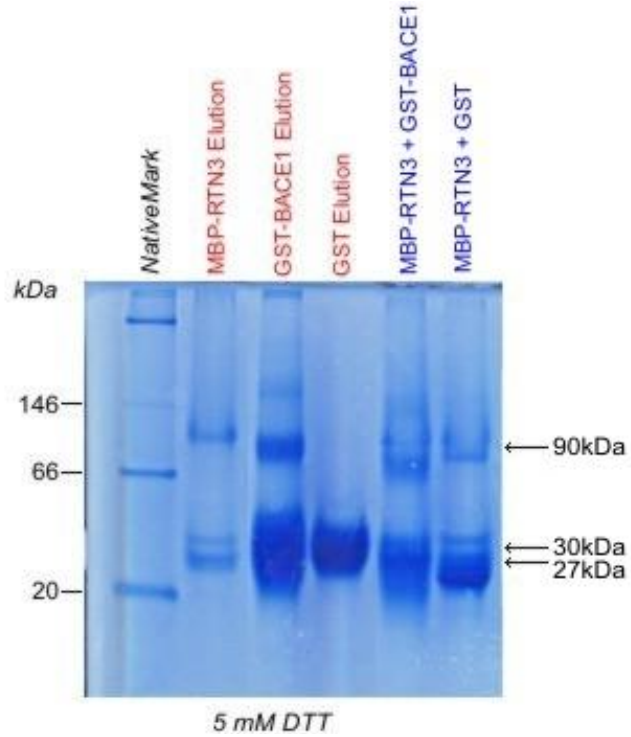

Figure 4.21. Native-PAGE of individual purifications *of MBP-RTN3 HD, GST-BACE1 and GST with addition of 5 mM DTT to all buffers. Overnight incubation at 37 °C (blue).*

Dithiothreitol (DTT) is a strong reducing agent, commonly used to reduce disulfide bonds of proteins via two sequential thiol-disulfide exchange reactions. Thus it is capable of disrupting protein folding and aggregation by preventing intramolecular and intermolecular disulfide bonds from forming between cysteine residues of proteins.

Compared to standard conditions (Figure 4.18) there were no differences detectable in MBP-RTN3 HD multimerisation (MBP-RTN3 Elution) when purified in the presence of DTT (Figure 4.21). As MBP-RTN3 HD does not contain any cysteine residues and methionine cannot form disulfide bonds, the complex may be stabilised by non-covalent hydrogen bonding or ionic interaction and these bonds could be solvent-inaccessible. Stronger denaturing conditions, such as addition of SDS in combination with β-mercaptoethanol and heat, caused these quaternary structures to disintegrate (Figure 4.14) and liberated MBP-RTN3 HD (48 kDa) and two smaller fragments. In the incubating samples MBP-RTN3 HD did not seem to interact with either GST-BACE1 or GST.

Multimerisation was also detected in purified GST-BACE1 samples (GST-BACE1 Elution), correlating to the observation made under standard conditions. Interestingly, GST alone showed no complex formation, suggesting that fused BACE1 could bury disulfide bonds of GST-BACE1 multimers which therefore cannot be reduced by DTT.

Overall, when employing high salt or strong reducing purification conditions no time or temperature dependence was observed in the behaviour of protein. Low salt conditions showed a temperature-dependent degradation of MBP-RTN3 HD multimers when incubated overnight at 37 °C.

CHAPTER 5

DISCUSSION

5.1. RTN3 in cell culture

In recent years Co-Immunoprecipitation (Co-IP) has become a common method to demonstrate the interaction between proteins, including transmembrane aspartic proteases such as BACE1 (*He et al., 2004; Murayama et al., 2006*). These protocols have employed various detergents to solubilise the cell membrane and extract the protein without thorough consideration of the mechanism of membrane disruption by detergents and the possible artefacts that could arise as a consequence of misuse.

When a low concentration of detergent is added to a membrane, the detergent molecules, comprising a hydrophobic tail and a hydrophilic head group, intercalate into the bilayer. The behaviour of the detergent is dependent on character and stereochemistry of the head group and tail (*Garavito and Ferguson-Miller, 2001*). The concentration of the detergent also plays an essential role. At a certain threshold, called the critical micelle concentration (CMC), detergent monomers self-associate and form micelles. Once the concentration surpasses the CMC, the detergent becomes able to solubilise hydrophobic and amphipathic molecules, such as lipids (*Rosen et al., 1978)* and even integral membrane proteins to create water-soluble protein-detergent complexes (*Garavito and Ferguson-Miller, 2001*). These mixed micelles vary considerably in structure and size depending on the type and concentration of the detergent used. The size of the micelle dictates the size of the membrane fragment and the proteins associated with it. At this stage it is crucial to chose carefully and balance possible effects of the detergent on the isolated protein. Numerous studies have used Triton X-100 as the benchmark detergent for similar studies, though it has been shown to give poor reproducibility between different experiments with the same starting material (*Lingwood and Simons, 2007*).

Variations in the size of the micelles may alter the yield or even cause a mixing of proteins that originally were located on different membrane areas (*Madore et al., 1999*). All this will have an impact on the Immunoprecipitation as well. It is indeed conceivable that two proteins localised in the same membrane region will Co-IP together although they do not necessarily bind directly to each other. Therefore, it is important to ascertain that protein-protein binding is genuine and not a result of artefacts made by the detergent.

To investigate whether BACE1 and RTN3 co-IPed together artefactually, it was decided to reconstitute the original approach published by He *et al.* (2004). In the published paper a HEK-293–derived stable cell line was used that expressed BACE1 tagged with hemagglutinin A (HA) at its C-terminus. To examine reticulon binding to BACE1, lysates from cells transfected with MYC-tagged RTN family members were prepared and a monoclonal antibody to HA was used for co-Immunoprecipitation, followed by western bot analysis with an antibody to the MYC-epitope of reticulon.

Since the detergents originally employed were not stated in the paper, conventional detergents such as NP-40 and Triton X-100 were selected for this study, which are most commonly used for solubilising membrane proteins. NP-40 has already been tested for reproducibility with RTN3 and BACE1 by Murayama *et al.* (2006). In order to verify the functional efficiency of BACE1-MYC over-expressing 5Y°s, all cells were lysed in a small scale trial using various concentrations of Triton X-100 and NP-40. Results were observed by Western Blot and confirmed that the applied detergent successfully liberated integral membrane proteins. The highest yield of protein was obtained using a concentration of 0.1 % Triton X-100. To test the interaction BACE-MYC 5Y°s were transfected with FLAG-RTN3 and the crude cell lysates examined using SDS-PAGE and Western Blot. Although BACE1-MYC was clearly visible on the gel at the calculated molecular weight, FLAG-RTN3 could not be detected, suggesting that it was not expressed properly. There are a number of reasons for low transfection efficiency including poor DNA quality, DNA degradation, time-dependent changes in the cell line or insufficient cell density due to excessive cell death. Attempts were made to optimise transfection conditions by varying Lipofectamine concentrations and using different antibodies(Table 3.12) but to no avail.

In conclusion, transfecting a BACE1-MYC stable cell line with FLAG-RTN3 did not show the anticipated protein-protein interaction. Consequently, the results obtained by He *et al.* (2004) could not be reproduced. Furthermore, it remained questionable if the detergents employed in their previous studies then promoted genuine binding between RTN3 and BACE1. Therefore an alternative approach was considered to reconstitute binding without the limiting effects of detergents.

5.2. Recombinant production of RTN3

In a novel approach it was decided to focus primarily on the predicted binding sites of both RTN3 and BACE1. The protein-protein interaction has been proposed to be mediated by a sequence in the RTN3 homology domain (RTN3 HD) and the C-terminal tail of BACE1, respectively. In this study the last 40 C-terminal amino acids of RTN3 were cloned, representing the C-terminal tail of the HD without loop or transmembrane regions (RTN3 HD). BACE1 was truncated to the C-terminal 24 amino acids. The main reason for this was to eliminate interference by different protein processing, such as folding or integration into the plasma membrane. If this interaction is stable it should be detectable using the minimal amino acid sequence of the predicted binding sites.

To this end, the gene encoding the RTN3 HD was successfully cloned into the expression vector pMal-c2x. Sequencing revealed that the RTN3 HD sequence in the expression vector aligned with the template DNA and the translated sequence was in frame with the maltose binding protein (MBP).

For binding studies a large quantity of purified protein is required. This requires that most recombinant protein is recovered in the liquid phase after cell lysis. MBP was used as a tag to artificially enhance solubility of the RTN3 HD fusion protein. *E. coli* MBP has been proven to be a more effective solubility partner than GST and thioredoxin proteins in a comparison of solubility enhancing properties (*Soerensen and Mortensen, 2005*). Nevertheless, the solubility of the fusion protein also depends on the properties of the recombinant partner and may therefore vary. Another reason to choose MBP-tagging was its high affinity for column-bound amylose which allows

one-step purification of the protein with a system readily available in the laboratory (see Protein Purification).

Once successful cloning of the gene was confirmed, competent *BL21-Codonplus(DE3)-RIL* cells were transformed with the expression vector pMal-c2x and induced to produce recombinant protein.

5.3. Protein purification

The MBP-RTN3 HD fusion protein was purified using an Amylose column with high affinity for MBP. The presented method proved to be an efficient and reproducible way to obtain an adequate quantity of the 48 kDa fusion protein, MBP-RTN3 HD, which was visualised by SDS-PAGE.

Purity of the elution fractions, however, was not fully achieved. A recurring observation by SDS-PAGE was the contamination of the elution fraction with two proteins with molecular weights of 45 and 38 kDa. These contaminants were detectable by immunoblotting with Anti-MBP and coomassie staining, suggesting they represent degraded products of MBP-RTN3 HD generated by strong denaturing conditions. In contrast, non-denaturing native gels showed contaminants at 25 and 30 kDa. Here, the majority of protein was represented by a higher molecular weight band at 90 kDa, which will be discussed below.

For future studies, additional methodologies should be considered to optimise purification and separate RTN3 HD from contaminants. Fast protein liquid chromatography (FPLC) is a method commonly used to isolate proteins in complex mixtures. This term is applied to several chromatography techniques. Depending on the preferred column it can separate macromolecules based on size (size exclusion), charge distribution (ion exchange), hydrophobicity, reverse-phase or biorecognition (affinity chromatography). Many of these techniques are identical to those carried out under high performance liquid chromatography (HPLC), however, the use of FPLC is typical for preparing large scale batches of a purified product. Each column contains small particles or gel beads known as the stationary phase. The sample is introduced into the injector and carried into the column by the liquid mobile phase. Once it

resides in the column, the mixture of proteins gets fractionated due to different components adhering to or diffusing into the gel.

In this study, size exclusion chromatography (SEC) would be a valuable method of separation. SEC is a gel filtration chromatography method, where proteins and polymers are fractionated based on their size and hydrodynamic volume. The protein is dissolved in an aqueous solvent and applied to a column packed with a matrix of porous polymer beads. Molecules smaller than the pore size can enter the particles and therefore have a longer transit time than larger molecules that will interact less with the stationary phase and thus elute faster. This method has further advantages in that it allows the preservation of biological activity since samples are applied under native conditions, leaving tertiary and quaternary structures intact. SEC measures the hydrodynamic volume or more specifically how much space a polymer molecule takes up in solution. Thus, it is also possible to distinguish folded and unfolded versions of the same protein. A 10 % difference in molecular mass is necessary to provide a good resolution. The technique can be combined with others that separate molecules by different characteristics, such as acidity, basicity, charge or affinity. Relevant bands were at 48 kDa (SDS-PAGE) and 90 kDa (native) with contaminants being considerably smaller and below 10 % difference. Therefore, affinity purification coupled with SEC would be effective in improving the isolation of MBP-RTN3 HD.

Considering the overall yield of MBP-RTN3 HD a sufficient quantity of protein could be isolated with the specified techniques. However, during the procedure the yield varied substantially. Despite the use of the highly hydrophilic MBP-tag, the protein was not entirely soluble and, following lysis, substantial amounts were still observed in the pellet. Over-expression of cloned genes in recombinant bacteria often induces the aggregation of protease-resistent misfolded protein to form so-called bacterial inclusion bodies (*Carrio and Villaverde, 2002*). This remains to be a major obstacle for protein production and *in vitro* recovery of functional protein often relies on complex re-folding procedures. The simultaneous co-expression of chaperone-encoding genes has also provided good results in a variety of studies with recombinant protein (*Caspers et al., 1994; Nishihara et al., 1998, 2000*). In particular the GroE proteins (*Richardson et al., 1998; Bukau et al., 1998*) have been shown to

accelerate the folding of MBP (*Sparrer et al., 1997*), consequently influencing solubility. The ability of MBP to promote the solubility of fusion partners can also be improved by addition of supplemental tags. Different configurations for MBP fusion proteins have been suggested for high-throughput protein expression and purification. According to *Routzahn et al.,* 2002, the most promising candidate appeared to be a fusion protein with a biotin acceptor peptide (BAP) on the N-terminus of MBP and/or a hexahistidine tag (His-tag) on the C-terminus of the passenger protein. However, due to the metal binding capacity of BACE1 (*Angeletti et al., 2005*) a His-tag for metal affinity chromatography was not suitable in this study.

5.4. RTN3 HD oligomerisation

Following purification, a prominent band of approximately 90 kDa was detected on all native gels. Surprisingly, native gels did not show the anticipated 48 kDa MBP-RTN3 HD monomer. It was concluded that the monomers instantly multimerised to form larger complexes. In accordance, dimers were calculated to migrate at 96 kDa.

The presence of RTN3 HD dimers is consistent with the observations published by He *et al.* (2006), where it was reported that RTN homo-dimerisation naturally occurs within cells. According to their findings, the reticulon homology domain appears to mediate this dimerisation, though the precise residues were not identified. In the experiments described here, the majority of RTN3 was present as a dimer under non-denaturing conditions.

In order to analyse how these multimers evolve, all proteins were prepared separately in strong reducing (DTT), high-salt or low-salt conditions. The addition of DTT did not disrupt MBP-RTN3 HD complexes, which confirms that dimerisation is not due to disulfide bonding. Thus the tertiary structure of MBP-RTN3 HD is dependent on non-covalent interactions, such as hydrogen or ionic bonding. The concentration of salt in the buffer was increased to characterise any ionic bonding. Although it was supposed to have a disrupting effect on ionic bonds, it did not alter the appearance of MBP-RTN3 HD dimers. Interestingly, low-salt conditions induced a significant increase in multimerisation at a higher molecular weight level. This dependency of multimerisation on a low level of ions provided in the solvent

environment suggests a distinct involvement of ionic bonds in the generation of RTN3 oligomers. Heat can be used to disrupt hydrogen bonds and non-polar hydrophobic interactions due to an increase in kinetic energy. SDS applies negative charge to amino acids and disrupts most non-disulfide-linked tertiary structures. A combination of SDS, heat and β-mercaptoethanol liberated the 48 kDa MBP-RTN3 HD monomer. However, these denaturing conditions were not employed to investigate binding.

5.5. Binding studies

Having successfully produced and purified MBP-RTN3 HD, methodologies were set up to investigate the proposed interaction between MBP-RTN3 HD and GST-BACE1. The first approach involved dual-purification of both proteins, a technique that combined purification and binding assay. The bacterial lysates of MBP-RTN3 HD and GST-BACE1 were sequentially applied to the same amylose column. Elution fractions were collected and observed by SDS-PAGE. Purified MBP-RTN3 HD was clearly visible at 48 kDa. However, the 30 kDa GST-BACE1 fusion protein could not be detected, despite being observed in the supernatant applied to the column. This demonstrates that protein-protein interaction did not take place on the affinity column. Accordingly, large quantities of GST-BACE1 were detected in the column flow through after being washed off the column.

An alternative approach employed the individual purification of MBP-RTN3 HD, GST-BACE1 and GST. The purified proteins were incubated together, in an equal ratio, to allow the binding-sites to interact. The purifications were varied by using strong reducing conditions, high salt or low salt concentrations. Purified fractions were combined under a variety of conditions, including different temperatures (37 °C and 17 °C) and time frames (1 hour, 12 hours). All samples were observed by SDS-PAGE and native gel to allow detection of the potential RTN3-BACE1 complex at a higher molecular weight. However, no additional bands were observed at the anticipated size (~78 kDa) and bands representing MBP-RTN3 HD, GST-BACE1 and GST were clearly separated from each other. Neither time nor temperature facilitated complex formation. Similarly, varying reducing conditions or salt concentrations did not seem to promote binding and the multimerisation detected in the purified elution

fractions remained precisely unchanged. As an exception, MBP-RTN3 HD purified using low-salt and incubated at 37 °C overnight, showed slightly less multimerisation compared to samples at 4 °C. This suggests a temperature-dependent dissociation of higher molecular weight multimers. In general, multimerisation was enhanced among all incubated protein purified at low-salt conditions, confirming the effect of salt on ionic bonding. However, it is doubtful that there is a connection between the low-salt induced generation and degradation of MBP-RTN3 HD multimers and the binding of RTN3 HD to BACE1.

In summary it is evident that, under these conditions, no stable protein-protein binding occurred between BACE1 and RTN3.

5.6. Possible reasons why GST-BACE1 and MBP-RTN3 HD failed to interact

Major advantages of prokaryotic recombinant protein expression systems include the availability of simple expression vectors and the ease at which they can be grown rapidly at high density on inexpensive substrates. Recombinant gene products will accumulate in *E. coli* at high levels in a full-length and biologically active form. Then again, over-production of heterologous proteins is sometimes accompanied by their misfolding and segregation into insoluble aggregates. A considerable quantity of protein may still be recovered from the post-lysis pellet. As protein is not secreted into the media but stays inside the cell, specific lysis techniques and purification systems are required to collect and separate functional protein from bacterial cell residues. In this study successful isolation was achieved by tagging the desired protein.

An important aspect in the use of recombinant systems is the absence of modification machinery in bacteria. Depending on the particular protein it may not be functional without specific post-translational modifications, potentially posing a dead-end to enzymatic studies. These modifications commonly include glycosylation or the addition of functional groups, support folding and are involved in structural changes of the protein. Above all they are involved in the formation of structural characteristics, affecting for example the generation of disulfide bonds. Therefore, it

is not advisable to use a recombinant expression system for proteins containing multiple disulfide bonds. This did not pose a problem since the truncated C-terminal tail of the RTN3 homology domain does not include any cysteine residues. Nevertheless, little is known about posttranslational modifications necessary for the functionality of RTN3 or the interaction with BACE1. In order to avoid problems of this kind a different expression vector could be used and the host cell changed. Insect or yeast cells rely on eukaryotic processing and can provide many of the key modifications as well as suitable secretory pathways to prevent the generation of inclusion bodies. Before deciding on a new host proteins should be treated with glycoside hydrolases such as Galactosidase to identify existing glycosylation patterns. Host cells should be selected accordingly to ensure their ability to provide the necessary posttranslational modifications.

The C-terminus of BACE1 has been shown by circular dichroism to have no significant secondary structural elements (R. Rose, in prep). However, there are cysteine residues in the area where the binding-site was proposed to be located. Covalent linkage between those residues could possibly bury or impede the binding-site. The addition of the reducing agent DTT during the purification of GST-BACE1, however, did not induce binding to RTN3. Thus it remains questionable if disulfide bonds are relevant in the inhibition of protein-protein interaction.

Another possible reason why interaction failed could be due to insufficient exposure of the binding sites. Although RTN3 was reduced to its terminal 40 amino acids, the number of amino acids may allow the generation of a secondary structure. However, a change in solvent conditions did not induce binding with BACE1 leaving it doubtful that binding sites could be uncovered by disrupting ionic or hydrophobic bonds. Accordingly, the MBP-tag is unlikely to manipulate the RTN3 binding-site as it is separated from RTN3 by a linker-domain and folds independently. To eliminate this in further studies it would be possible to cleave MBP from the fusion protein using the specific protease Factor Xa.

A remaining question is the influence of MBP-RTN3 HD dimerisation observed on native gels. As mentioned before the majority of MBP-RTN3 HD is present in the form of a dimer, unless denaturing conditions are employed that would disrupt any

bonding between RTN3 and BACE1 as well. This raises the question whether dimerisation may possibly interfere with the RTN3-BACE1 binding-site. *He et al.* reported that C-terminally deleted RTN3 variants (minus 36 amino acids) lacking the QID motive were not able to bind BACE1 but would still form dimers with RTN3. It is therefore likely that dimerisation is mediated by a different region within the HD than binding to BACE1. However, a significant influence may still exist and further investigations are necessary to determine exactly which regions on RTN3 HD are responsible for dimerisation.

5.7. Conclusion

Due to time constraints it was not possible to investigate further and apply all of the mentioned amendments. Nevertheless, current data illustrates that the published interaction between RTN3 and BACE1 could be an artefact of the IP method and the indiscriminate use of detergents. It is evident that reconstitution of the proposed interaction between RTN3 and BACE1 using recombinant protein was not possible. Hence, it is essential to continue investigations and explore alternative strategies, such as the recombinant approach employed in this study. The challenging hunt for novel therapeutic approaches, in particular the modulation of BACE1 activity by protease inhibitors, has been demanding but promising so far. Any insights gained in function and distinctive features of RTN3 or BACE1 as well as being able to draw connections to AD pathogenesis might be more than valuable in the search for new small molecule therapeutics.

BIBLIOGRAPHY

ALLINSON, T. M., PARKIN, E. T., TURNER, A. J. & HOOPER, N. M. 2003. ADAMs family members as amyloid precursor protein alpha-secretases. *J Neurosci Res,* 74**,** 342-52.

ANGELETTI, B., WALDRON, K. J., FREEMAN, K. B., BAWAGAN, H., HUSSAIN, I., MILLER, C. C., LAU, K. F., TENNANT, M. E., DENNISON, C., ROBINSON, N. J. & DINGWALL, C. 2005. BACE1 cytoplasmic domain interacts with the copper chaperone for superoxide dismutase-1 and binds copper. *J Biol Chem,* 280**,** 17930-7.

ANNAERT, W. & DE STROOPER, B. 2002. A cell biological perspective on Alzheimer's disease. *Annu Rev Cell Dev Biol,* 18**,** 25-51.

BARTUS, R. T., DEAN, R. L., 3RD, BEER, B. & LIPPA, A. S. 1982. The cholinergic hypothesis of geriatric memory dysfunction. *Science,* 217**,** 408-14.

BASI, G., FRIGON, N., BARBOUR, R., DOAN, T., GORDON, G., MCCONLOGUE, L., SINHA, S. & ZELLER, M. 2003. Antagonistic effects of beta-site amyloid precursor protein-cleaving enzymes 1 and 2 on beta-amyloid peptide production in cells. *J Biol Chem,* 278**,** 31512-20.

BENJANNET, S., ELAGOZ, A., WICKHAM, L., MAMARBACHI, M., MUNZER, J. S., BASAK, A., LAZURE, C., CROMLISH, J. A., SISODIA, S., CHECLER, F., CHRETIEN, M. & SEIDAH, N. G. 2001. Post-translational processing of beta-secretase (beta-amyloid-converting enzyme) and its ectodomain shedding. The pro- and transmembrane/cytosolic domains affect its cellular activity and amyloid-beta production. *J Biol Chem,* 276**,** 10879-87.

BODENDORF, U., DANNER, S., FISCHER, F., STEFANI, M., STURCHLER-PIERRAT, C., WIEDERHOLD, K. H., STAUFENBIEL, M. & PAGANETTI, P.

2002. Expression of human beta-secretase in the mouse brain increases the steady-state level of beta-amyloid. *J Neurochem,* 80**,** 799-806.

BROOKMEYER, R., JOHNSON, E., ZIEGLER-GRAHAM, K. & ARRIGHI, H. M. 2007. Forecasting the global burden of Alzheimer's disease. *Alzheimers Dement,* 3**,** 186-91.

BUKAU, B. & HORWICH, A. L. 1998. The Hsp70 and Hsp60 chaperone machines. *Cell,* 92**,** 351-66.

CAI, H., WANG, Y., MCCARTHY, D., WEN, H., BORCHELT, D. R., PRICE, D. L. & WONG, P. C. 2001. BACE1 is the major beta-secretase for generation of Abeta peptides by neurons. *Nat Neurosci,* 4**,** 233-4.

CAMPION, D., BRICE, A., DUMANCHIN, C., PUEL, M., BAULAC, M., DE LA SAYETTE, V., HANNEQUIN, D., DUYCKAERTS, C., MICHON, A., MARTIN, C., MOREAU, V., PENET, C., MARTINEZ, M., CLERGET-DARPOUX, F., AGID, Y. & FREBOURG, T. 1996. A novel presenilin 1 mutation resulting in familial Alzheimer's disease with an onset age of 29 years. *Neuroreport,* 7**,** 1582-4.

CARRIO, M. M. & VILLAVERDE, A. 2002. Construction and deconstruction of bacterial inclusion bodies. *J Biotechnol,* 96**,** 3-12.

CASPERS, P., STIEGER, M. & BURN, P. 1994. Overproduction of bacterial chaperones improves the solubility of recombinant protein tyrosine kinases in Escherichia coli. *Cell Mol Biol (Noisy-le-grand),* 40**,** 635-44.

CHARLWOOD, J., DINGWALL, C., MATICO, R., HUSSAIN, I., JOHANSON, K., MOORE, S., POWELL, D. J., SKEHEL, J. M., RATCLIFFE, S., CLARKE, B., TRILL, J., SWEITZER, S. & CAMILLERI, P. 2001. Characterization of the glycosylation profiles of Alzheimer's beta -secretase protein Asp-2 expressed in a variety of cell lines. *J Biol Chem,* 276**,** 16739-48.

CHEN, M. S., HUBER, A. B., VAN DER HAAR, M. E., FRANK, M., SCHNELL, L., SPILLMANN, A. A., CHRIST, F. & SCHWAB, M. E. 2000. Nogo-A is a myelin-associated neurite outgrowth inhibitor and an antigen for monoclonal antibody IN-1. *Nature,* 403**,** 434-9.

CITRON, M. 2004. Strategies for disease modification in Alzheimer's disease. *Nat Rev Neurosci,* 5**,** 677-85.

DAVIES, P. & MALONEY, A. J. 1976. Selective loss of central cholinergic neurons in Alzheimer's disease. *Lancet,* 2**,** 1403.

DE STROOPER, B. & ANNAERT, W. 2000. Proteolytic processing and cell biological functions of the amyloid precursor protein. *J Cell Sci,* 113 (Pt 11)**,** 1857-70.

DILLEN, K. & ANNAERT, W. 2006. A two decade contribution of molecular cell biology to the centennial of Alzheimer's disease: are we progressing toward therapy? *Int Rev Cytol,* 254**,** 215-300.

DINGWALL, C. 2001. Spotlight on BACE: the secretases as targets for treatment in Alzheimer disease. *J Clin Invest,* 108**,** 1243-6.

DRACHMAN, D. A. & LEAVITT, J. 1974. Human memory and the cholinergic system. A relationship to aging? *Arch Neurol,* 30**,** 113-21.

FISCHER, F., MOLINARI, M., BODENDORF, U. & PAGANETTI, P. 2002. The disulphide bonds in the catalytic domain of BACE are critical but not essential for amyloid precursor protein processing activity. *J Neurochem,* 80**,** 1079-88.

FOURNIER, A. E., GRANDPRE, T. & STRITTMATTER, S. M. 2001. Identification of a receptor mediating Nogo-66 inhibition of axonal regeneration. *Nature,* 409**,** 341-6.

FRANCIS, P. T., PALMER, A. M., SNAPE, M. & WILCOCK, G. K. 1999. The cholinergic hypothesis of Alzheimer's disease: a review of progress. *J Neurol Neurosurg Psychiatry,* 66**,** 137-47.

FUKUMOTO, H., CHEUNG, B. S., HYMAN, B. T. & IRIZARRY, M. C. 2002. Beta-secretase protein and activity are increased in the neocortex in Alzheimer disease. *Arch Neurol,* 59**,** 1381-9.

GARAVITO, R. M. & FERGUSON-MILLER, S. 2001. Detergents as tools in membrane biochemistry. *J Biol Chem,* 276**,** 32403-6.

GOEDERT, M., KLUG, A. & CROWTHER, R. A. 2006. Tau protein, the paired helical filament and Alzheimer's disease. *J Alzheimers Dis,* 9**,** 195-207.

GOEDERT, M., SPILLANTINI, M. G. & CROWTHER, R. A. 1991. Tau proteins and neurofibrillary degeneration. *Brain Pathol,* 1**,** 279-86.

GOLDGABER, D., LERMAN, M. I., MCBRIDE, O. W., SAFFIOTTI, U. & GAJDUSEK, D. C. 1987. Characterization and chromosomal localization of a cDNA encoding brain amyloid of Alzheimer's disease. *Science,* 235**,** 877-80.

HARDY, J. & SELKOE, D. J. 2002. The amyloid hypothesis of Alzheimer's disease: progress and problems on the road to therapeutics. *Science,* 297**,** 353-6.

HE, W., HU, X., SHI, Q., ZHOU, X., LU, Y., FISHER, C. & YAN, R. 2006. Mapping of interaction domains mediating binding between BACE1 and RTN/Nogo proteins. *J Mol Biol,* 363**,** 625-34.

HE, W., LU, Y., QAHWASH, I., HU, X. Y., CHANG, A. & YAN, R. 2004. Reticulon family members modulate BACE1 activity and amyloid-beta peptide generation. *Nat Med,* 10**,** 959-65.

HE, W., SHI, Q., HU, X. & YAN, R. 2007. The membrane topology of RTN3 and its effect on binding of RTN3 to BACE1. *J Biol Chem,* 282**,** 29144-51.

HESTON, L. L., MASTRI, A. R., ANDERSON, V. E. & WHITE, J. 1981. Dementia of the Alzheimer type. Clinical genetics, natural history, and associated conditions. *Arch Gen Psychiatry,* 38**,** 1085-90.

HOLSINGER, R. M., MCLEAN, C. A., BEYREUTHER, K., MASTERS, C. L. & EVIN, G. 2002. Increased expression of the amyloid precursor beta-secretase in Alzheimer's disease. *Ann Neurol,* 51**,** 783-6.

HU, X., SHI, Q., ZHOU, X., HE, W., YI, H., YIN, X., GEARING, M., LEVEY, A. & YAN, R. 2007. Transgenic mice overexpressing reticulon 3 develop neuritic abnormalities. *EMBO J,* 26**,** 2755-67.

HUSSAIN, I., CHRISTIE, G., SCHNEIDER, K., MOORE, S. & DINGWALL, C. 2001. Prodomain processing of Asp1 (BACE2) is autocatalytic. *J Biol Chem,* 276**,** 23322-8.

HUSSAIN, I., POWELL, D., HOWLETT, D. R., TEW, D. G., MEEK, T. D., CHAPMAN, C., GLOGER, I. S., MURPHY, K. E., SOUTHAN, C. D., RYAN, D. M., SMITH, T. S., SIMMONS, D. L., WALSH, F. S., DINGWALL, C. & CHRISTIE, G. 1999. Identification of a novel aspartic protease (Asp 2) as beta-secretase. *Mol Cell Neurosci,* 14**,** 419-27.

HUSSAIN, I., POWELL, D. J., HOWLETT, D. R., CHAPMAN, G. A., GILMOUR, L., MURDOCK, P. R., TEW, D. G., MEEK, T. D., CHAPMAN, C., SCHNEIDER, K., RATCLIFFE, S. J., TATTERSALL, D., TESTA, T. T., SOUTHAN, C., RYAN, D. M., SIMMONS, D. L., WALSH, F. S., DINGWALL, C. & CHRISTIE,

G. 2000. ASP1 (BACE2) cleaves the amyloid precursor protein at the beta-secretase site. *Mol Cell Neurosci,* 16**,** 609-19.

IQBAL, K., ALONSO ADEL, C., CHEN, S., CHOHAN, M. O., EL-AKKAD, E., GONG, C. X., KHATOON, S., LI, B., LIU, F., RAHMAN, A., TANIMUKAI, H. & GRUNDKE-IQBAL, I. 2005. Tau pathology in Alzheimer disease and other tauopathies. *Biochim Biophys Acta,* 1739**,** 198-210.

JARRETT, J. T., BERGER, E. P. & LANSBURY, P. T., JR. 1993. The carboxy terminus of the beta amyloid protein is critical for the seeding of amyloid formation: implications for the pathogenesis of Alzheimer's disease. *Biochemistry,* 32**,** 4693-7.

KAETHER, C., HAASS, C. & STEINER, H. 2006. Assembly, trafficking and function of gamma-secretase. *Neurodegener Dis,* 3**,** 275-83.

KALVODOVA, L., KAHYA, N., SCHWILLE, P., EHEHALT, R., VERKADE, P., DRECHSEL, D. & SIMONS, K. 2005. Lipids as modulators of proteolytic activity of BACE: involvement of cholesterol, glycosphingolipids, and anionic phospholipids in vitro. *J Biol Chem,* 280**,** 36815-23.

KANG, J., LEMAIRE, H. G., UNTERBECK, A., SALBAUM, J. M., MASTERS, C. L., GRZESCHIK, K. H., MULTHAUP, G., BEYREUTHER, K. & MULLER-HILL, B. 1987. The precursor of Alzheimer's disease amyloid A4 protein resembles a cell-surface receptor. *Nature,* 325**,** 733-6.

KIMURA, T., HAMADA, Y., STOCHAJ, M., IKARI, H., NAGAMINE, A., ABDEL-RAHMAN, H., IGAWA, N., HIDAKA, K., NGUYEN, J. T., SAITO, K., HAYASHI, Y. & KISO, Y. 2006. Design and synthesis of potent beta-secretase (BACE1) inhibitors with P1' carboxylic acid bioisosteres. *Bioorg Med Chem Lett,* 16**,** 2380-6.

KOO, E. H. 2002. The beta-amyloid precursor protein (APP) and Alzheimer's disease: does the tail wag the dog? *Traffic,* 3**,** 763-70.

LEVY-LAHAD, E., WASCO, W., POORKAJ, P., ROMANO, D. M., OSHIMA, J., PETTINGELL, W. H., YU, C. E., JONDRO, P. D., SCHMIDT, S. D., WANG, K. & ET AL. 1995. Candidate gene for the chromosome 1 familial Alzheimer's disease locus. *Science,* 269**,** 973-7.

LING, Y., MORGAN, K. & KALSHEKER, N. 2003. Amyloid precursor protein (APP) and the biology of proteolytic processing: relevance to Alzheimer's disease. *Int J Biochem Cell Biol,* 35**,** 1505-35.

LINGWOOD, D. & SIMONS, K. 2007. Detergent resistance as a tool in membrane research. *Nat Protoc,* 2**,** 2159-65.

LUO, Y., BOLON, B., KAHN, S., BENNETT, B. D., BABU-KHAN, S., DENIS, P., FAN, W., KHA, H., ZHANG, J., GONG, Y., MARTIN, L., LOUIS, J. C., YAN, Q., RICHARDS, W. G., CITRON, M. & VASSAR, R. 2001. Mice deficient in BACE1, the Alzheimer's beta-secretase, have normal phenotype and abolished beta-amyloid generation. *Nat Neurosci,* 4**,** 231-2.

MADORE, N., SMITH, K. L., GRAHAM, C. H., JEN, A., BRADY, K., HALL, S. & MORRIS, R. 1999. Functionally different GPI proteins are organized in different domains on the neuronal surface. *EMBO J,* 18**,** 6917-26.

MURAYAMA, K. S., KAMETANI, F., SAITO, S., KUME, H., AKIYAMA, H. & ARAKI, W. 2006. Reticulons RTN3 and RTN4-B/C interact with BACE1 and inhibit its ability to produce amyloid beta-protein. *Eur J Neurosci,* 24**,** 1237-44.

NILSSON, L., NORDBERG, A., HARDY, J., WESTER, P. & WINBLAD, B. 1986. Physostigmine restores 3H-acetylcholine efflux from Alzheimer brain slices to normal level. *J Neural Transm,* 67**,** 275-85.

NISHIHARA, K., KANEMORI, M., KITAGAWA, M., YANAGI, H. & YURA, T. 1998. Chaperone coexpression plasmids: differential and synergistic roles of DnaK-DnaJ-GrpE and GroEL-GroES in assisting folding of an allergen of Japanese cedar pollen, Cryj2, in Escherichia coli. *Appl Environ Microbiol,* 64**,** 1694-9.

NISHIHARA, K., KANEMORI, M., YANAGI, H. & YURA, T. 2000. Overexpression of trigger factor prevents aggregation of recombinant proteins in Escherichia coli. *Appl Environ Microbiol,* 66**,** 884-9.

OERTLE, T., KLINGER, M., STUERMER, C. A. & SCHWAB, M. E. 2003a. A reticular rhapsody: phylogenic evolution and nomenclature of the RTN/Nogo gene family. *FASEB J,* 17**,** 1238-47.

OERTLE, T., VAN DER HAAR, M. E., BANDTLOW, C. E., ROBEVA, A., BURFEIND, P., BUSS, A., HUBER, A. B., SIMONEN, M., SCHNELL, L., BROSAMLE, C., KAUPMANN, K., VALLON, R. & SCHWAB, M. E. 2003b. Nogo-A inhibits

neurite outgrowth and cell spreading with three discrete regions. *J Neurosci,* 23**,** 5393-406.

PERICAK-VANCE, M. A., BEBOUT, J. L., GASKELL, P. C., JR., YAMAOKA, L. H., HUNG, W. Y., ALBERTS, M. J., WALKER, A. P., BARTLETT, R. J., HAYNES, C. A., WELSH, K. A. & ET AL. 1991. Linkage studies in familial Alzheimer disease: evidence for chromosome 19 linkage. *Am J Hum Genet,* 48**,** 1034-50.

PERRY, E. K., GIBSON, P. H., BLESSED, G., PERRY, R. H. & TOMLINSON, B. E. 1977. Neurotransmitter enzyme abnormalities in senile dementia. Choline acetyltransferase and glutamic acid decarboxylase activities in necropsy brain tissue. *J Neurol Sci,* 34**,** 247-65.

PRICE, D. L., TANZI, R. E., BORCHELT, D. R. & SISODIA, S. S. 1998. Alzheimer's disease: genetic studies and transgenic models. *Annu Rev Genet,* 32**,** 461-93.

PROKOP, S., SHIROTANI, K., EDBAUER, D., HAASS, C. & STEINER, H. 2004. Requirement of PEN-2 for stabilization of the presenilin N-/C-terminal fragment heterodimer within the gamma-secretase complex. *J Biol Chem,* 279**,** 23255-61.

PUIG, O., CASPARY, F., RIGAUT, G., RUTZ, B., BOUVERET, E., BRAGADO-NILSSON, E., WILM, M. & SERAPHIN, B. 2001. The tandem affinity purification (TAP) method: a general procedure of protein complex purification. *Methods,* 24**,** 218-29.

QUERFURTH, H. W. & LAFERLA, F. M. 2010. Alzheimer's disease. *N Engl J Med,* 362**,** 329-44.

RICHARDSON, A., LANDRY, S. J. & GEORGOPOULOS, C. 1998. The ins and outs of a molecular chaperone machine. *Trends Biochem Sci,* 23**,** 138-43.

ROBAKIS, N. K., RAMAKRISHNA, N., WOLFE, G. & WISNIEWSKI, H. M. 1987. Molecular cloning and characterization of a cDNA encoding the cerebrovascular and the neuritic plaque amyloid peptides. *Proc Natl Acad Sci U S A,* 84**,** 4190-4.

ROBERDS, S. L., ANDERSON, J., BASI, G., BIENKOWSKI, M. J., BRANSTETTER, D. G., CHEN, K. S., FREEDMAN, S. B., FRIGON, N. L., GAMES, D., HU, K., JOHNSON-WOOD, K., KAPPENMAN, K. E., KAWABE, T. T., KOLA, I., KUEHN, R., LEE, M., LIU, W., MOTTER, R., NICHOLS, N. F., POWER, M.,

ROBERTSON, D. W., SCHENK, D., SCHOOR, M., SHOPP, G. M., SHUCK, M. E., SINHA, S., SVENSSON, K. A., TATSUNO, G., TINTRUP, H., WIJSMAN, J., WRIGHT, S. & MCCONLOGUE, L. 2001. BACE knockout mice are healthy despite lacking the primary beta-secretase activity in brain: implications for Alzheimer's disease therapeutics. *Hum Mol Genet,* 10**,** 1317-24.

ROSEN, M. J. 1978. *Surfactants and interfacial phenomena,* New York, Wiley.

ROUTZAHN, K. M. & WAUGH, D. S. 2002. Differential effects of supplementary affinity tags on the solubility of MBP fusion proteins. *J Struct Funct Genomics,* 2**,** 83-92.

RYLETT, R. J., BALL, M. J. & COLHOUN, E. H. 1983. Evidence for high affinity choline transport in synaptosomes prepared from hippocampus and neocortex of patients with Alzheimer's disease. *Brain Res,* 289**,** 169-75.

SCHEUNER, D., ECKMAN, C., JENSEN, M., SONG, X., CITRON, M., SUZUKI, N., BIRD, T. D., HARDY, J., HUTTON, M., KUKULL, W., LARSON, E., LEVY-LAHAD, E., VIITANEN, M., PESKIND, E., POORKAJ, P., SCHELLENBERG, G., TANZI, R., WASCO, W., LANNFELT, L., SELKOE, D. & YOUNKIN, S. 1996. Secreted amyloid beta-protein similar to that in the senile plaques of Alzheimer's disease is increased in vivo by the presenilin 1 and 2 and APP mutations linked to familial Alzheimer's disease. *Nat Med,* 2**,** 864-70.

SCHMECHEL, D. E., SAUNDERS, A. M., STRITTMATTER, W. J., CRAIN, B. J., HULETTE, C. M., JOO, S. H., PERICAK-VANCE, M. A., GOLDGABER, D. & ROSES, A. D. 1993. Increased amyloid beta-peptide deposition in cerebral cortex as a consequence of apolipoprotein E genotype in late-onset Alzheimer disease. *Proc Natl Acad Sci U S A,* 90**,** 9649-53.

SCHOLEFIELD, Z., YATES, E. A., WAYNE, G., AMOUR, A., MCDOWELL, W. & TURNBULL, J. E. 2003. Heparan sulfate regulates amyloid precursor protein processing by BACE1, the Alzheimer's beta-secretase. *J Cell Biol,* 163**,** 97-107.

SELKOE, D. J. 2001. Alzheimer's disease: genes, proteins, and therapy. *Physiol Rev,* 81**,** 741-66.

SHERRINGTON, R., ROGAEV, E. I., LIANG, Y., ROGAEVA, E. A., LEVESQUE, G., IKEDA, M., CHI, H., LIN, C., LI, G., HOLMAN, K. & ET AL. 1995. Cloning of a gene bearing missense mutations in early-onset familial Alzheimer's disease. *Nature,* 375**,** 754-60.

SINHA, S., ANDERSON, J. P., BARBOUR, R., BASI, G. S., CACCAVELLO, R., DAVIS, D., DOAN, M., DOVEY, H. F., FRIGON, N., HONG, J., JACOBSON-CROAK, K., JEWETT, N., KEIM, P., KNOPS, J., LIEBERBURG, I., POWER, M., TAN, H., TATSUNO, G., TUNG, J., SCHENK, D., SEUBERT, P., SUOMENSAARI, S. M., WANG, S., WALKER, D., ZHAO, J., MCCONLOGUE, L. & JOHN, V. 1999. Purification and cloning of amyloid precursor protein beta-secretase from human brain. *Nature,* 402**,** 537-40.

SPARRER, H., RUTKAT, K. & BUCHNER, J. 1997. Catalysis of protein folding by symmetric chaperone complexes. *Proc Natl Acad Sci U S A,* 94**,** 1096-100.

STRITTMATTER, W. J., SAUNDERS, A. M., SCHMECHEL, D., PERICAK-VANCE, M., ENGHILD, J., SALVESEN, G. S. & ROSES, A. D. 1993. Apolipoprotein E: high-avidity binding to beta-amyloid and increased frequency of type 4 allele in late-onset familial Alzheimer disease. *Proc Natl Acad Sci U S A,* 90**,** 1977-81.

TANZI, R. E., GUSELLA, J. F., WATKINS, P. C., BRUNS, G. A., ST GEORGE-HYSLOP, P., VAN KEUREN, M. L., PATTERSON, D., PAGAN, S., KURNIT, D. M. & NEVE, R. L. 1987. Amyloid beta protein gene: cDNA, mRNA distribution, and genetic linkage near the Alzheimer locus. *Science,* 235**,** 880-4.

TANZI, R. E., VAULA, G., ROMANO, D. M., MORTILLA, M., HUANG, T. L., TUPLER, R. G., WASCO, W., HYMAN, B. T., HAINES, J. L., JENKINS, B. J. & ET AL. 1992. Assessment of amyloid beta-protein precursor gene mutations in a large set of familial and sporadic Alzheimer disease cases. *Am J Hum Genet,* 51**,** 273-82.

VASSAR, R. 2001. The beta-secretase, BACE: a prime drug target for Alzheimer's disease. *J Mol Neurosci,* 17**,** 157-70.

VASSAR, R. 2002. Beta-secretase (BACE) as a drug target for Alzheimer's disease. *Adv Drug Deliv Rev,* 54**,** 1589-602.

VASSAR, R. 2004. BACE1: the beta-secretase enzyme in Alzheimer's disease. *J Mol Neurosci,* 23**,** 105-14.

VASSAR, R., BENNETT, B. D., BABU-KHAN, S., KAHN, S., MENDIAZ, E. A., DENIS, P., TEPLOW, D. B., ROSS, S., AMARANTE, P., LOELOFF, R., LUO, Y., FISHER, S., FULLER, J., EDENSON, S., LILE, J., JAROSINSKI, M. A., BIERE, A. L., CURRAN, E., BURGESS, T., LOUIS, J. C., COLLINS, F., TREANOR, J., ROGERS, G. & CITRON, M. 1999. Beta-secretase cleavage of Alzheimer's amyloid precursor protein by the transmembrane aspartic protease BACE. *Science,* 286**,** 735-41.

WAKANA, Y., KOYAMA, S., NAKAJIMA, K., HATSUZAWA, K., NAGAHAMA, M., TANI, K., HAURI, H. P., MELANCON, P. & TAGAYA, M. 2005. Reticulon 3 is involved in membrane trafficking between the endoplasmic reticulum and Golgi. *Biochem Biophys Res Commun,* 334**,** 1198-205.

WHITEHOUSE, P. J., PRICE, D. L., STRUBLE, R. G., CLARK, A. W., COYLE, J. T. & DELON, M. R. 1982. Alzheimer's disease and senile dementia: loss of neurons in the basal forebrain. *Science,* 215**,** 1237-9.

YAN, R., BIENKOWSKI, M. J., SHUCK, M. E., MIAO, H., TORY, M. C., PAULEY, A. M., BRASHIER, J. R., STRATMAN, N. C., MATHEWS, W. R., BUHL, A. E., CARTER, D. B., TOMASSELLI, A. G., PARODI, L. A., HEINRIKSON, R. L. & GURNEY, M. E. 1999. Membrane-anchored aspartyl protease with Alzheimer's disease beta-secretase activity. *Nature,* 402**,** 533-7.

YAN, R., MUNZNER, J. B., SHUCK, M. E. & BIENKOWSKI, M. J. 2001. BACE2 functions as an alternative alpha-secretase in cells. *J Biol Chem,* 276**,** 34019-27.

YAN, R., SHI, Q., HU, X. & ZHOU, X. 2006. Reticulon proteins: emerging players in neurodegenerative diseases. *Cell Mol Life Sci,* 63**,** 877-89.

YANG, L. B., LINDHOLM, K., YAN, R., CITRON, M., XIA, W., YANG, X. L., BEACH, T., SUE, L., WONG, P., PRICE, D., LI, R. & SHEN, Y. 2003. Elevated beta-secretase expression and enzymatic activity detected in sporadic Alzheimer disease. *Nat Med,* 9**,** 3-4.

YANG, Y. S. & STRITTMATTER, S. M. 2007. The reticulons: a family of proteins with diverse functions. *Genome Biol,* 8**,** 234.

ZHENG, H. & KOO, E. H. 2006. The amyloid precursor protein: beyond amyloid. *Mol Neurodegener,* 1**,** 5.

CURRICULUM VITAE

Personal Information

Address Ohlsdorferstraße 2, 4810 Gmunden, Austria
Telephone +43 699 10801633
Email christine.weber@gmx.at
Date of Birth 13 June 1985

Education

2003 - 2010 **Mag. Pharmacy**
UNIVERSITY OF VIENNA, Faculty of Life Sciences, Austria

1995 - 2003 **Grammar school**
BUNDESGYMNASIUM GMUNDEN, Austria

Scientific experience

2010 **Internship at AOP Orphan Pharmaceuticals** (3 months)

2010 **Tutor in drug analysis and development** (1 month)
INSTITUTE OF MEDICINAL CHEMISTRY, University of Vienna

2009 **Tutor in drug analysis and development** (1 month)
INSTITUTE OF MEDICINAL CHEMISTRY, University of Vienna

2008 - 2009 **Erasmus student** (4 months)
KING'S COLLEGE LONDON, Pharmaceutical Science Division
Diploma thesis titled "Investigations into the interaction between the β-secretase protein BACE1 and a member of the reticulon family, RTN3".

2008 **Internship in radiopharmacy**
VIENNA GENERAL HOSPITAL, Department of Nuclear Medicine, Radiopharmaceutical Sciences

Scholarships

- Erasmus Scholarship (EU Lifelong Learning Programme), October 2008 – January 2009